Electronic Supplementary Material (ESI) for Nanoscale.

S1 Studied systems

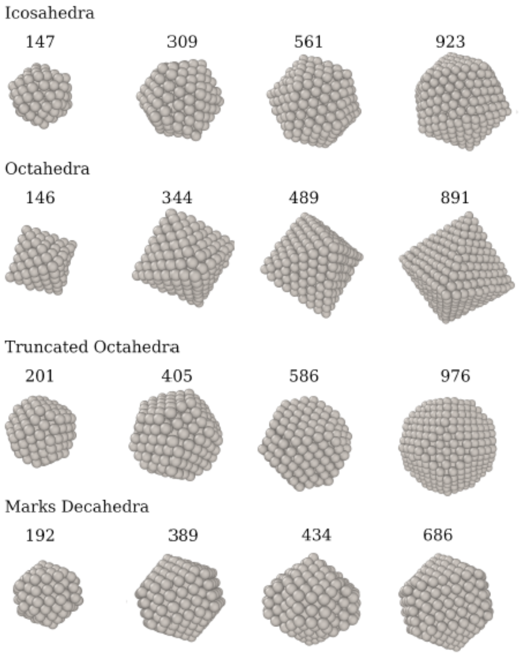

		Diameter (nm)					
Shape	N atoms	Ag	Au	Cu	Ni	Pd	Pt
Oh	146	2.04	2.04	1.81	1.51	1.66	1.96
Ih	147	1.74	1.73	1.53	1.49	1.65	1.66
MDh	192	1.82	1.81	1.61	1.57	1.73	1.74
TOh	201	1.83	1.82	1.62	1.57	1.74	1.75
Ih	309	2.31	2.31	2.04	1.99	2.20	2.22
Oh	344	2.86	2.85	2.53	2.46	2.72	2.74
MDh	389	2.37	2.36	2.10	2.04	2.25	2.27
TOh	405	2.38	2.37	2.11	2.05	2.27	2.28
MDh	434	2.56	2.55	2.27	2.21	2.44	2.46
Oh	489	3.27	3.26	2.90	2.82	3.11	3.13
Ih	561	2.89	2.89	2.55	2.49	2.75	2.77
TOh	586	2.74	2.73	2.43	2.36	2.61	2.63
MDh	686	2.92	2.91	2.58	2.51	2.78	2.80
Oh	891	4.09	4.07	3.62	3.52	3.89	3.92
Ih	923	3.47	3.46	3.06	2.99	3.30	3.32
TOh	976	3.30	3.28	2.92	2.84	3.14	3.16

Figure S1: Left side: Snapshots of all the isomers considered in this investigation plotted with Ovito. The name of each morphology is reported per each row. The correspondence between nanoparticle size in atoms and diameter (nm) is given on the table in the right side.

Figure S1 lists the initial structures grouped in their geometrical family, i.e. icosahedra (Ih), octahedra (Oh), truncated octahedra (To), and Marks decahedra (MDh, where the reentrance p is fixed to two atoms corresponding to the smallest possible reentrance). Per each of them the size in terms of total number of atoms is given, while on the right we report a conversion between number of atoms, shape and the diameter (in nm), defined as the maximum existing distance between a pair of atoms. Summarising we have explored the 1.5 - 4.1 nm range. We also note that asymmetry might end in 'longer' diameters although the number of atoms is smaller. We suggest to not simply convert number of atoms and diameter using the ratio between the volume of a spherical object and its atomic volume, as $N_{NP} d_{at}^3 \propto d_{NP}^3$, where d_{at} is twice the atomic radius. For example, a Oh_{891} made of Ag would result in a diameter of 2.77 nm instead of 4.09 nm from the distance between its vertexes.

S2 Pair distance distribution function binning

Figure S4 shows the average pair distance distribution functions of a Pt nanoparticle of 201 atoms at different temperatures for different choices of the binning width. For the case of a bin width larger or equal than 0.5Å the peak in the PDDF at the second neighbour distance is not observed. We thus establish this bin width as the largest that can be used for discriminating between melted and solid nanoparticles from their PDDF characterization. The choice for bin width we report in the main text is anyway smaller, 0.05Å.

We note that given enough statistics also smaller bin widths are suitable, Figs S3 and S2 . Similar trends are observed for the case of the systems with different size, initial shape and composition considered during this investigation.

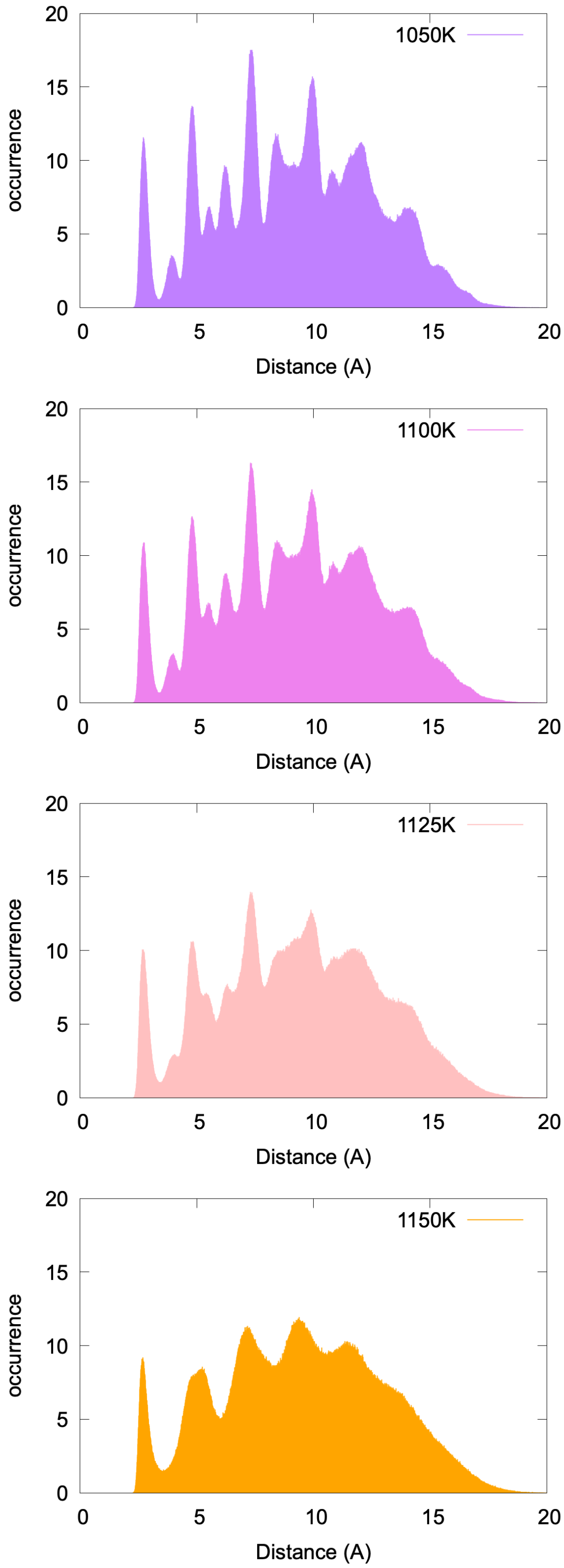

Figure S2: Pair distance distribution functions temperature evolution plotted according to a distance binning of 0.005Å size

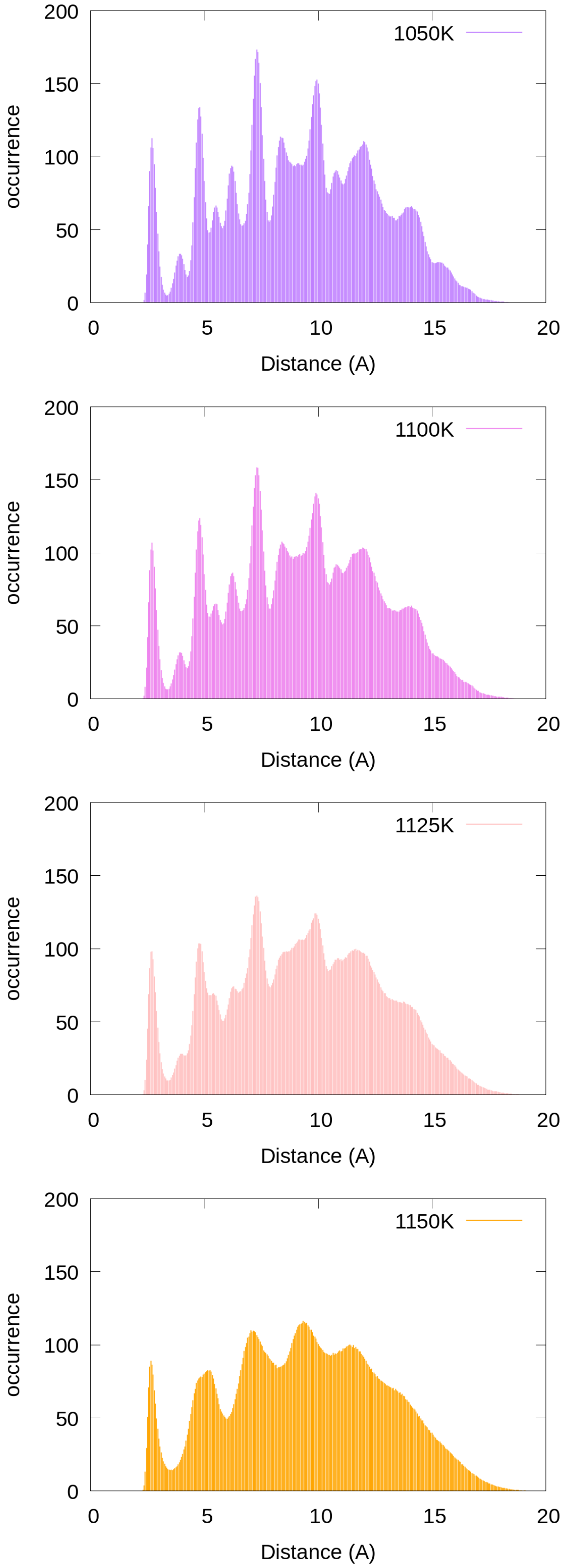

Figure S3: Pair distance distribution functions temperature evolution plotted according to a distance binning of 0.05Å size

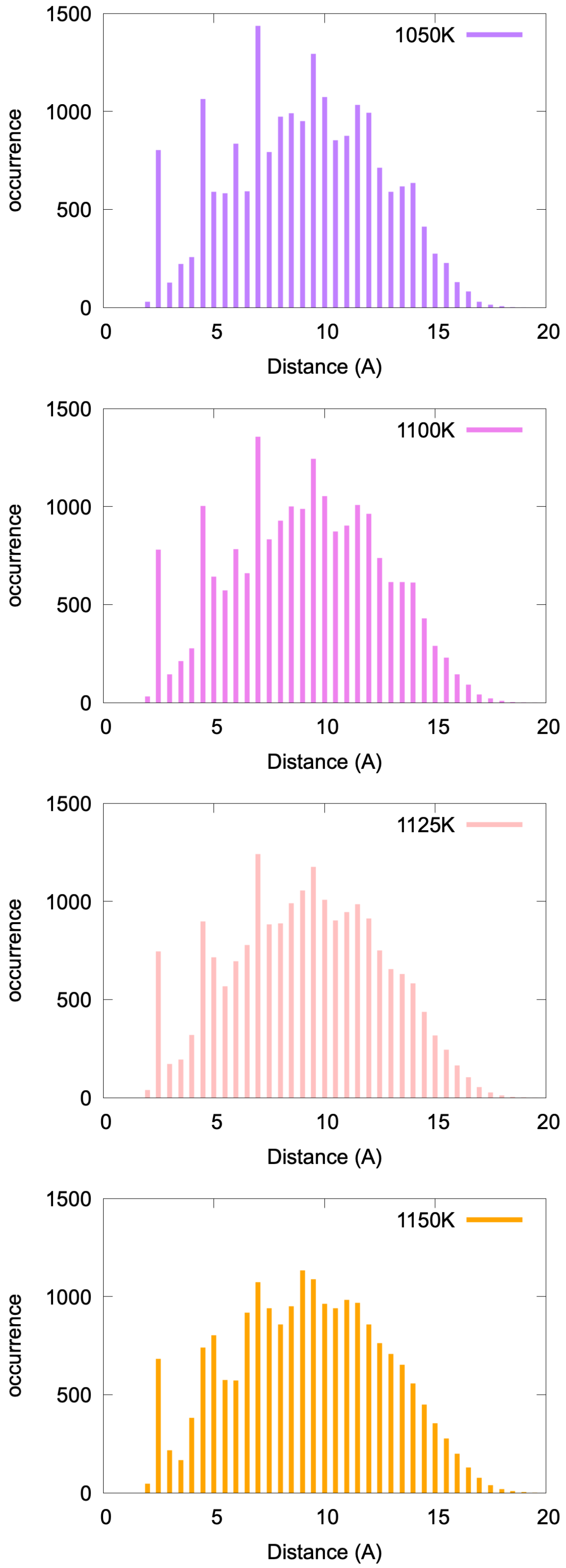

Figure S4: Pair distance distribution functions temperature evolution plotted according to a distance binning of 0.5Å size

S3 Maximum PDDF Evolution

This section showcases some case studies which exemplify the robustness of the PDDF peak analysis to identify the melting of anisotropic nanoparticles.

In Figure S5 we show the temperature dependent evolution of the excess energy (red), KL(h|c) (green), maximum PDDF distance (blue), and specific heat (black) in Pt nanoparticles with an initial morphology corresponding to a large Octahedra.

We later corroborated this analysis in the case of Pt nanorods, Figure S6. Only four independent simulations are averaged in this case. The set up of these simulations is reported in [Phys. Chem. Chem. Phys., 2019,21, 4888-4898]

These examples show that the maximum PDDF distance is not a universal order parameter to estimate the melting point in metallic nanoparticles. Indeed prior to the melting, signalled by the largest peak in the heat capacity, the anisotropic nanoparticles undergo strong rearrangements leading to a diminished radius. Nevertheless, let us stress here that the PDDF KL estimate is not affected by such rearrangement.

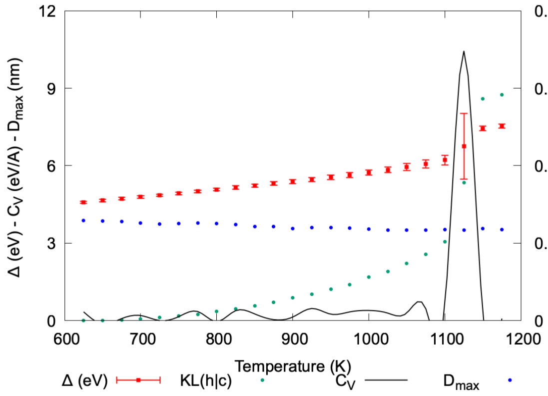

Figure S5: Temperature dependent evolution of the excess energy (red), KL(h|c) (green), maximum PDDF distance (blue), and specific heat (black) in Pt Octahedra of 891 atoms.

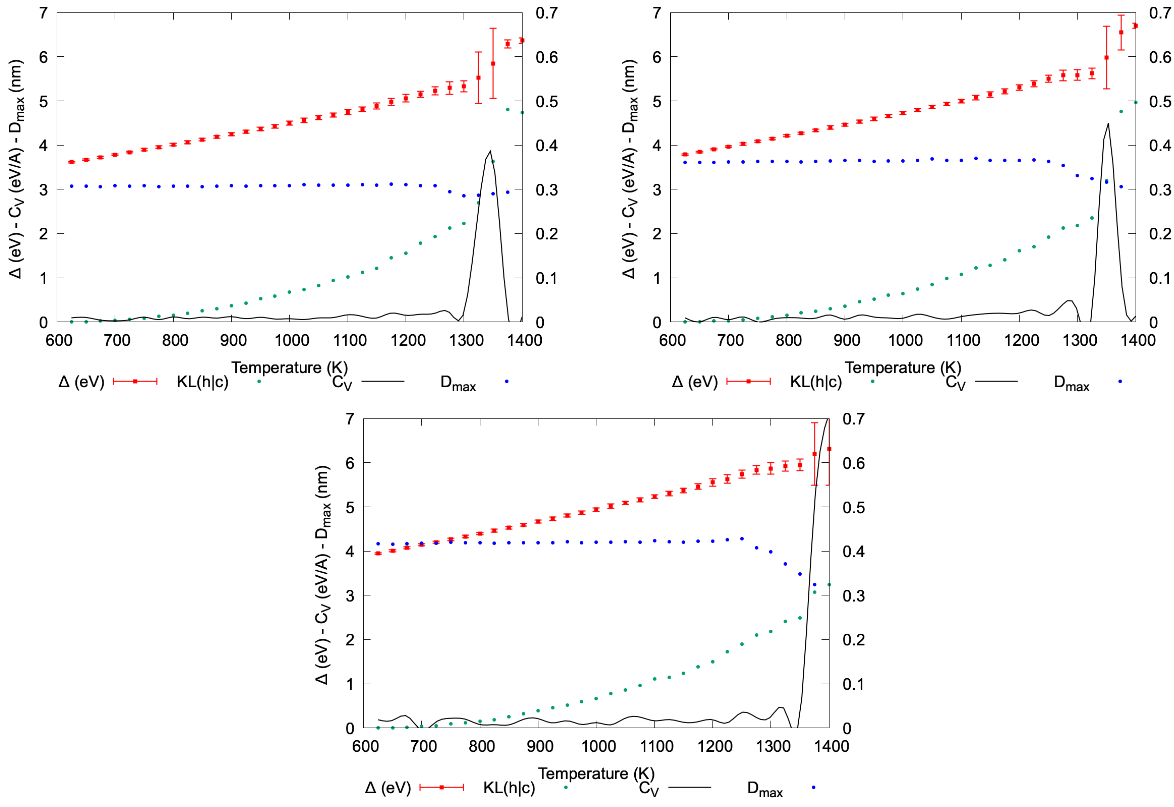

Figure S6: Temperature dependent evolution of the excess energy (red), KL(h|c) (green), maximum PDDF distance (blue), and specific heat (black) in Pt nanorods of 522 (top), 644 (center), 766 (bottom) atoms.

S4 Pair distance distribution function temperature evolution

In this section we report five different snapshots of the average PDDF of each investigated system at different temperatures. The structural characteristics, e.g. the presence of twin planes and five-fold symmetry axis, can be observed in the pair distance distribution function of solid ”magic sizes”. The formation of thermally driven surface defects, surface peeling through adatom diffusion and/or exchanges contribute to the increased loss of order in the distribution of longer pair distances. While local first nearest neighbour shells average distance is essentially fixed, a stronger disorder is evident in the second and third nearest neighbour shell. Consequently while the first nearest neighbour peak displays a more and more broadened profile for increasingly high temperatures, the peak at the second nearest neighbour disappears at melting. Temperatures in the caption are given in K.

S4.1 Platinum

Figure S7: PDDF temperature evolution in Pt systems with size from 146 to 405 atoms. Temperature-color coding follows as blue = 950, cyan = 1075, green = 1200, yellow = 1325, red = 1450

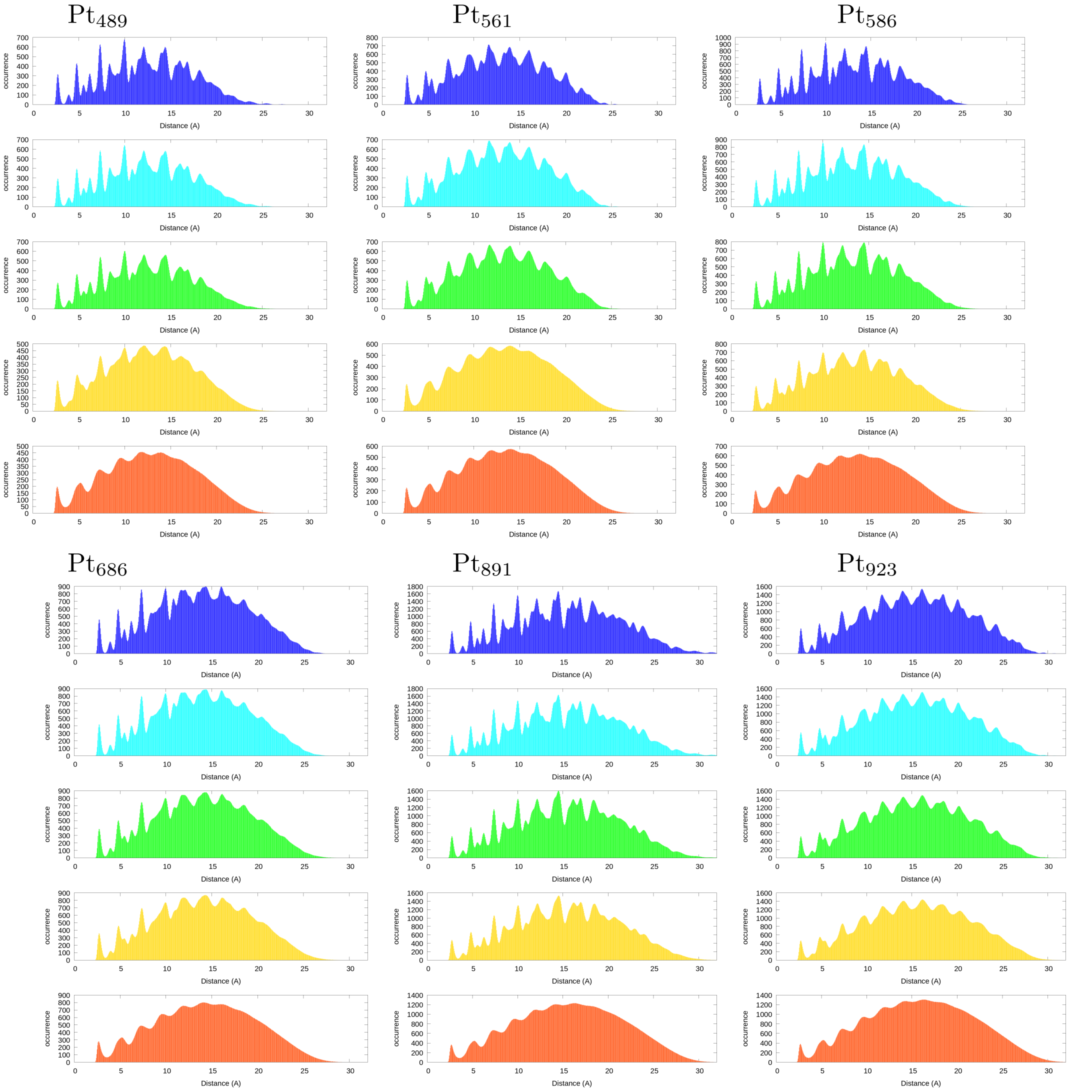

Figure S8: PDDF temperature evolution in Pt systems with size from 489 to 923 atoms. Temperature-color coding follows as blue = 950, cyan = 1075, green = 1200, yellow = 1325, red = 1450

S4.2 Gold

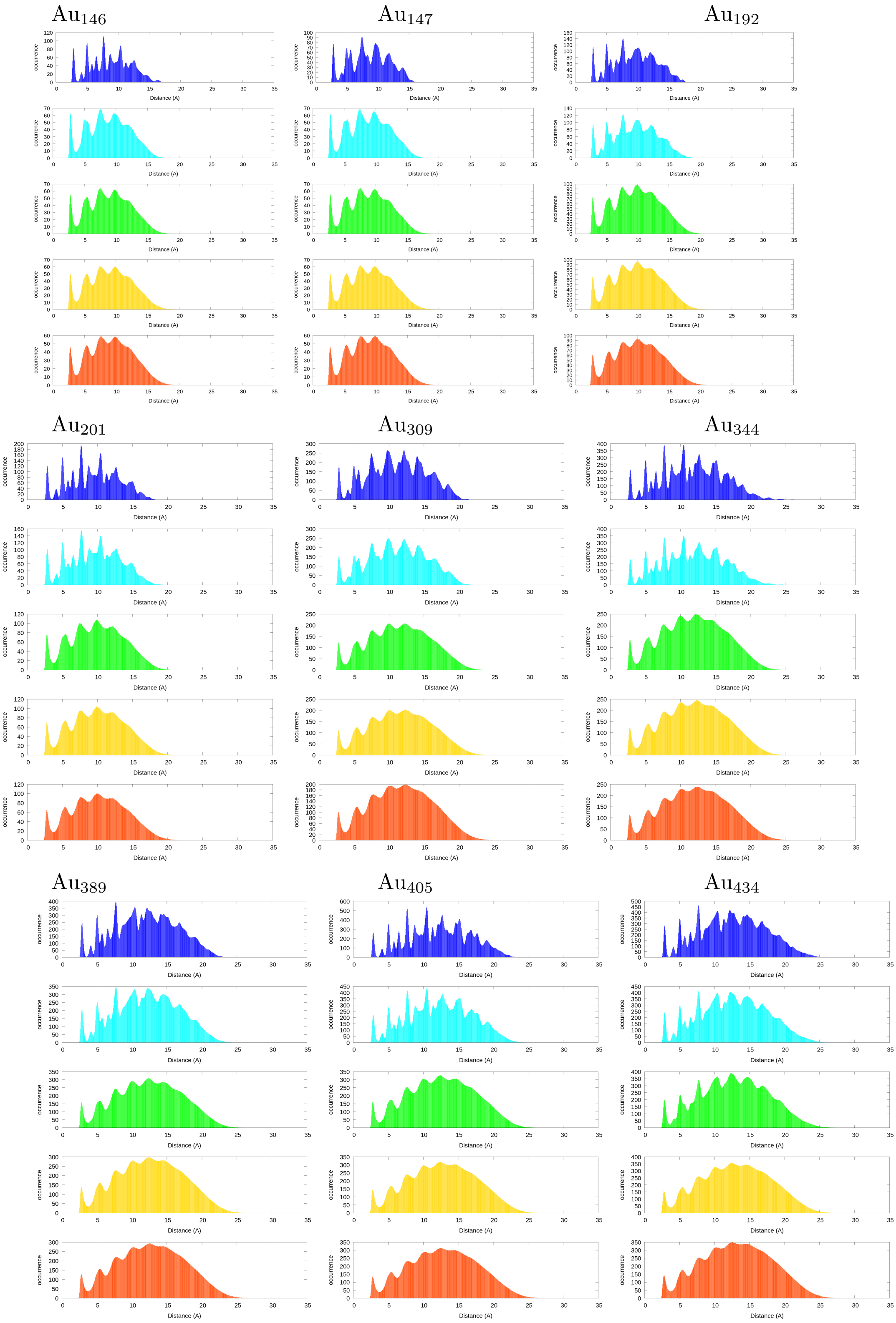

Figure S9: PDDF temperature evolution in Au systems with size from 146 to 405 atoms.Temperature-color coding follows as blue = 450, cyan = 675, green = 800, yellow = 925, red = 1050.

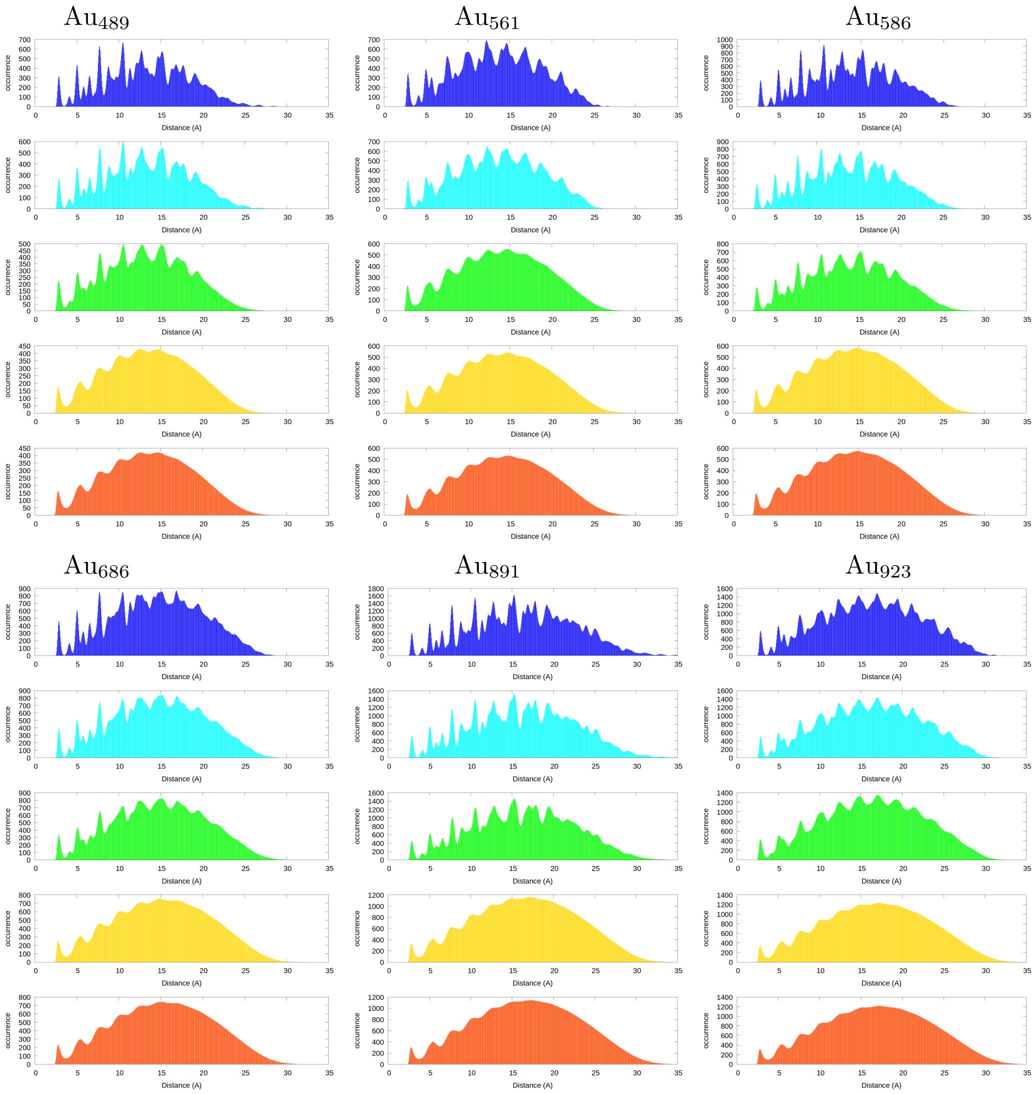

Figure S10: PDDF temperature evolution in Au systems with size from 489 to 923 atoms. Temperature-color coding follows as blue = 450, cyan = 675, green = 800, yellow = 925, red = 1050.

S4.3 Silver

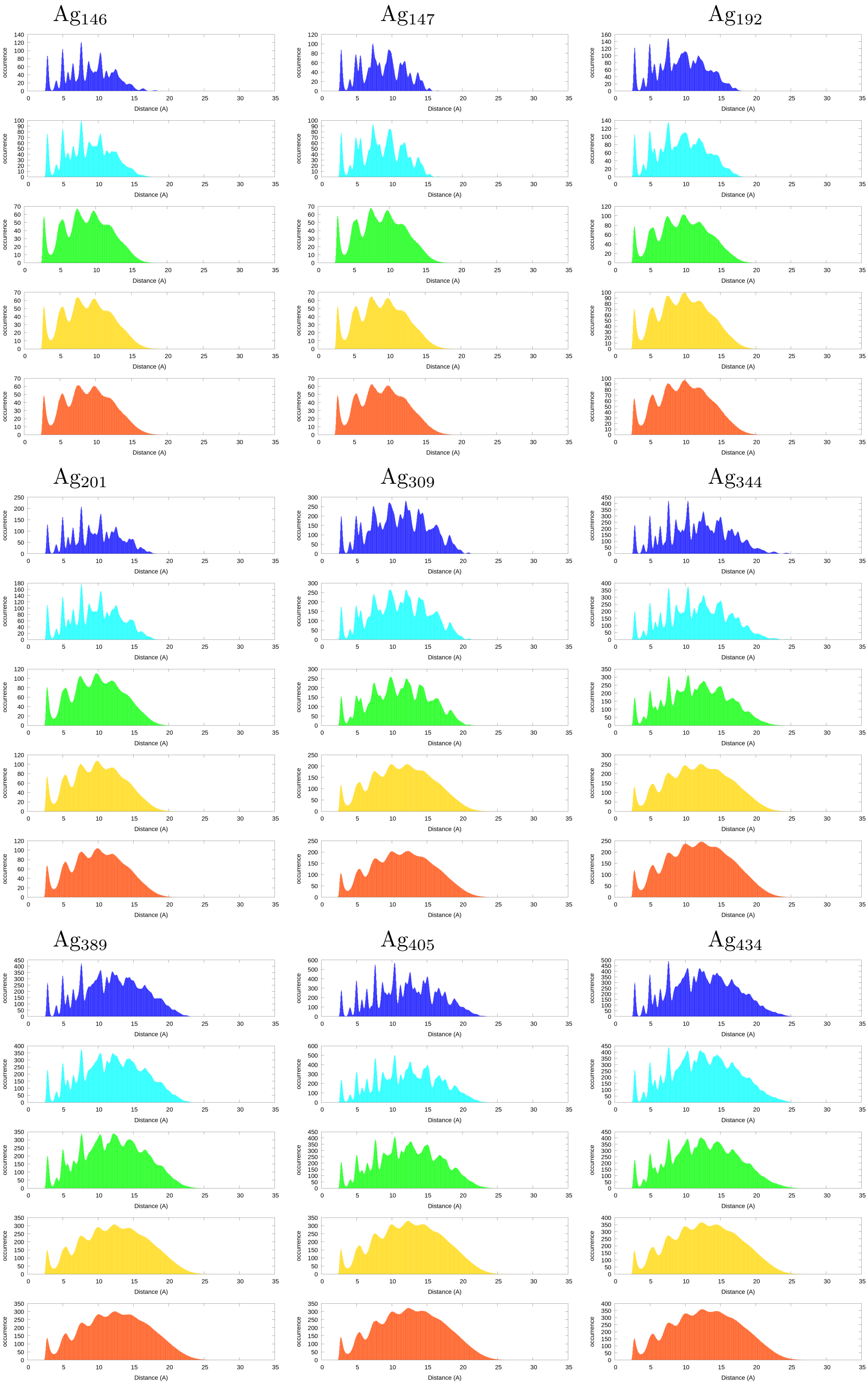

Figure S11: PDDF temperature evolution in Ag systems with size from 146 to 405 atoms. Temperature-color coding follows as blue = 450, cyan = 675, green = 800, yellow = 925, red = 1050.

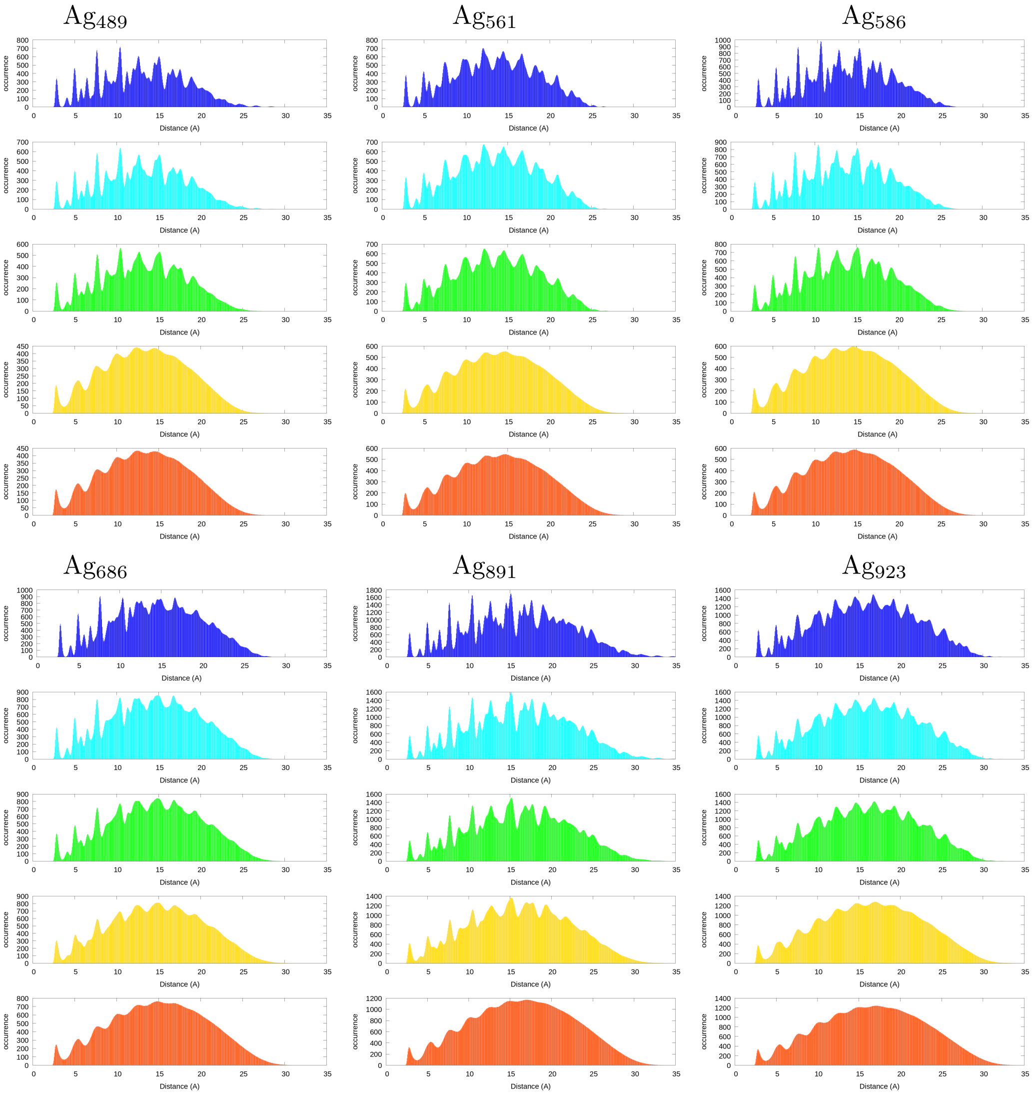

Figure S12: PDDF temperature evolution in Ag systems with size from 489 to 923 atoms. Temperature-color coding follows as blue = 450, cyan = 675, green = 800, yellow = 925, red = 1050.

S4.4 Nickel

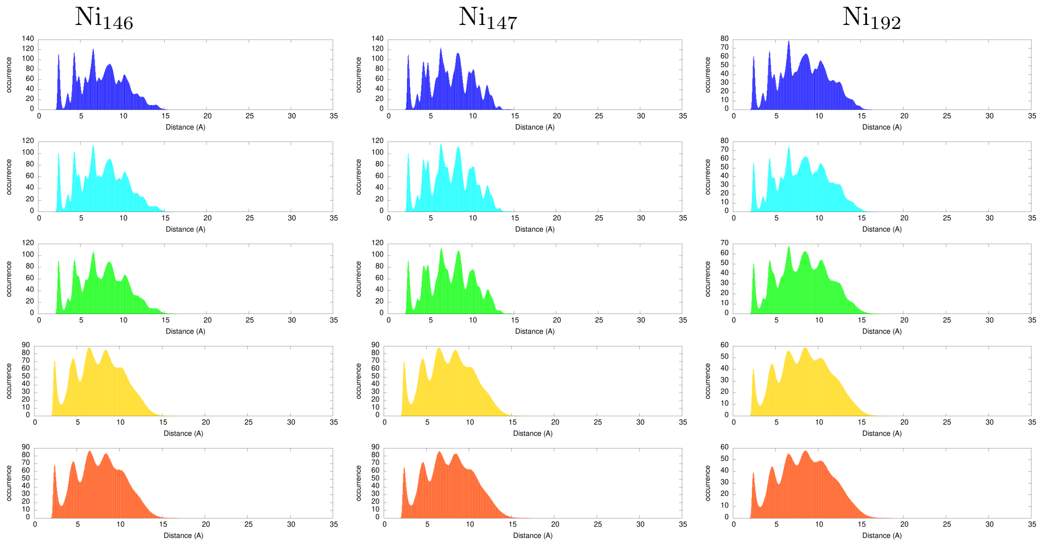

Figure S13: PDDF temperature evolution in Ni systems with size from 146 to 192 atoms. Temperature-color coding for sizes 146 and 147 follows blue = 725, cyan = 850, green = 975, yellow = 1175, red = 1250. Size 192 follows blue = 825, cyan = 925, green = 1050, yellow = 1175, red = 1275.

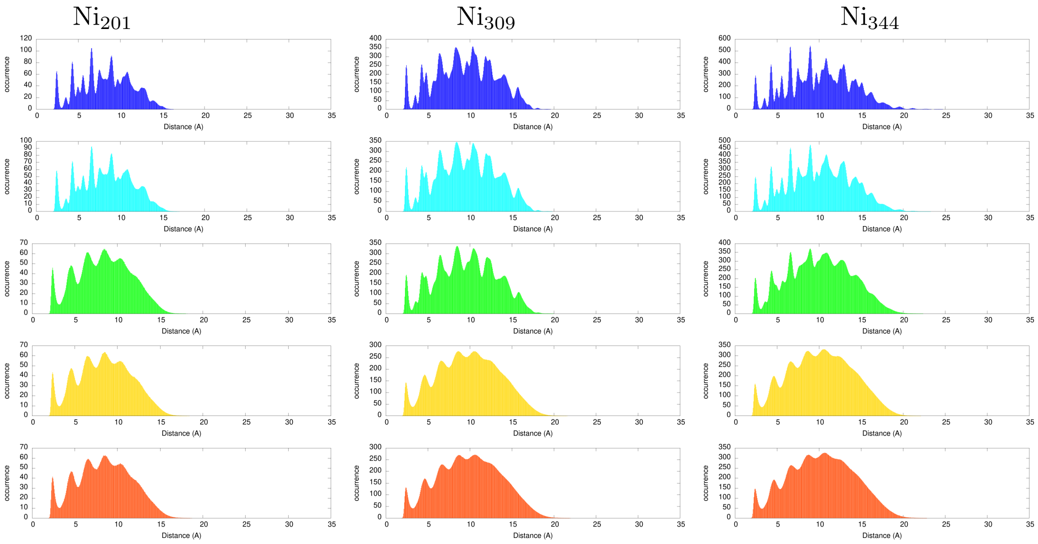

Figure S14: PDDF temperature evolution in Ni systems with size from 201 to 344 atoms. Temperature-color coding for size 201 follows blue = 825, cyan = 925, green = 1050, yellow = 1175, red = 1275. Sizes 309 and 344 follow blue = 725, cyan = 925, green = 1125, yellow = 1350, red = 1575.

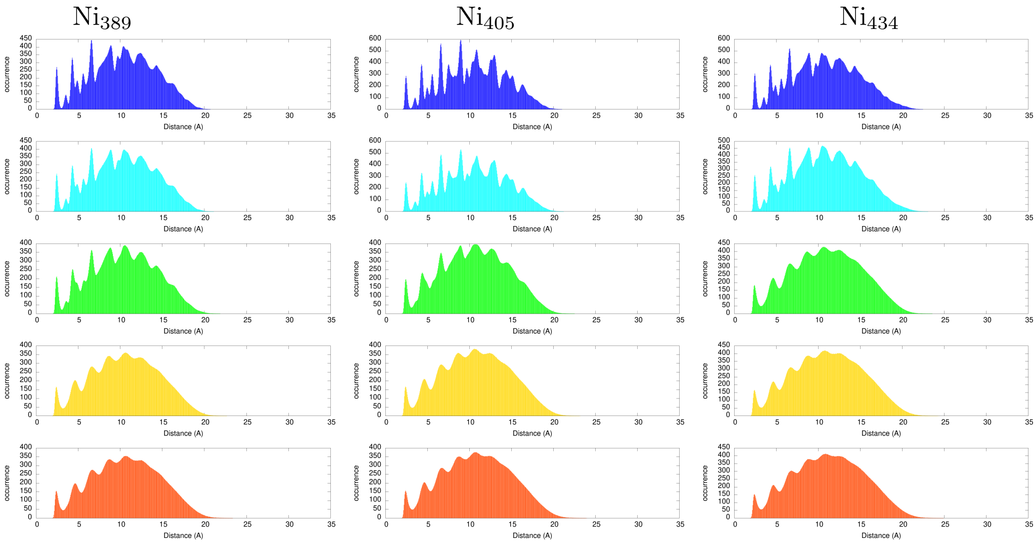

Figure S15: PDDF temperature evolution in Ni systems with size from 389 to 434 atoms. Temperature-color coding for size 389 follows blue = 825, cyan = 975, green = 1125, yellow = 1275, red = 1425. Size 405 follows blue = 825, cyan = 1000, green = 1175, yellow = 1350, red = 1525. Size 434 follows blue = 825, cyan = 1050, green = 1300, yellow = 1550, red = 1775.

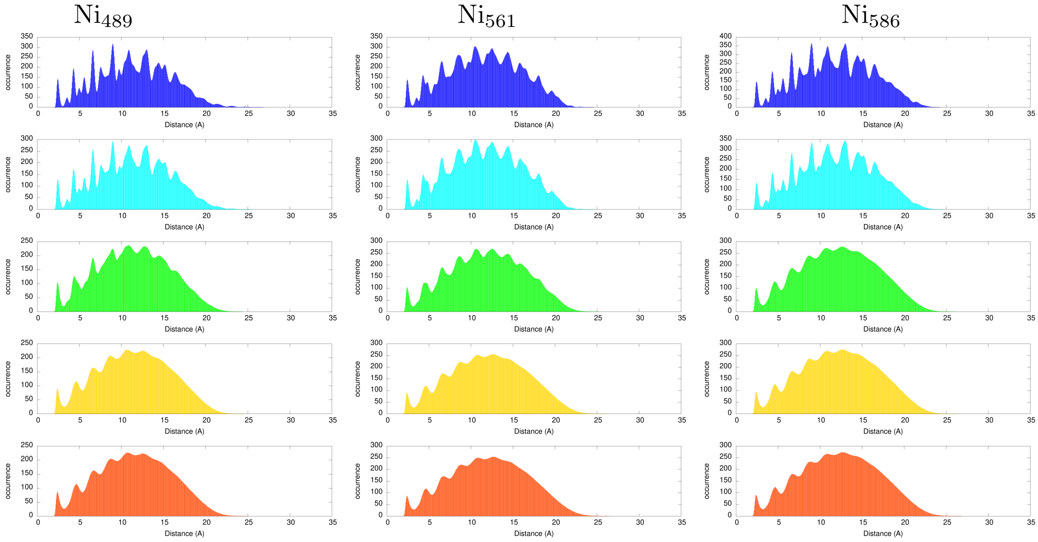

Figure S16: PDDF temperature evolution in Ni systems with size from 489 to 586 atoms. Temperature-color coding for size 489 follows blue = 925, cyan = 1050, green = 1200, yellow = 1350, red = 1475. Sizes 561 and 586 follow blue = 1025, cyan = 1175, green = 1300, yellow = 1450, red = 1575.

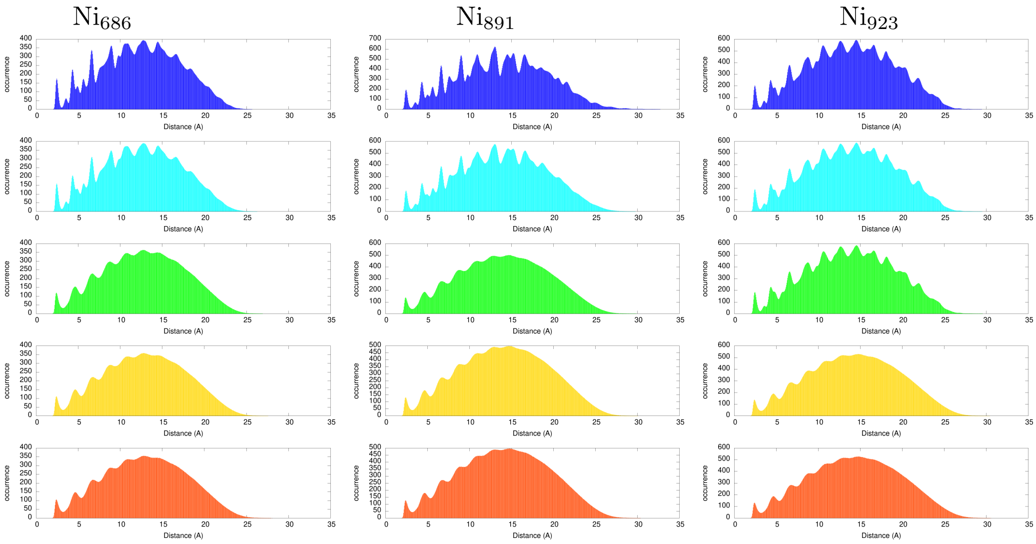

Figure S17: PDDF temperature evolution in Ni systems with size from 686 to 923 atoms. Temperature-color coding for sizes 686 and 923 follows blue = 1025, cyan = 1175, green = 1300, yellow = 1450, red = 1575. Size 923 follows blue = 1125, cyan = 1225, green = 1275, yellow = 1450, red = 1575.

S4.5 Copper

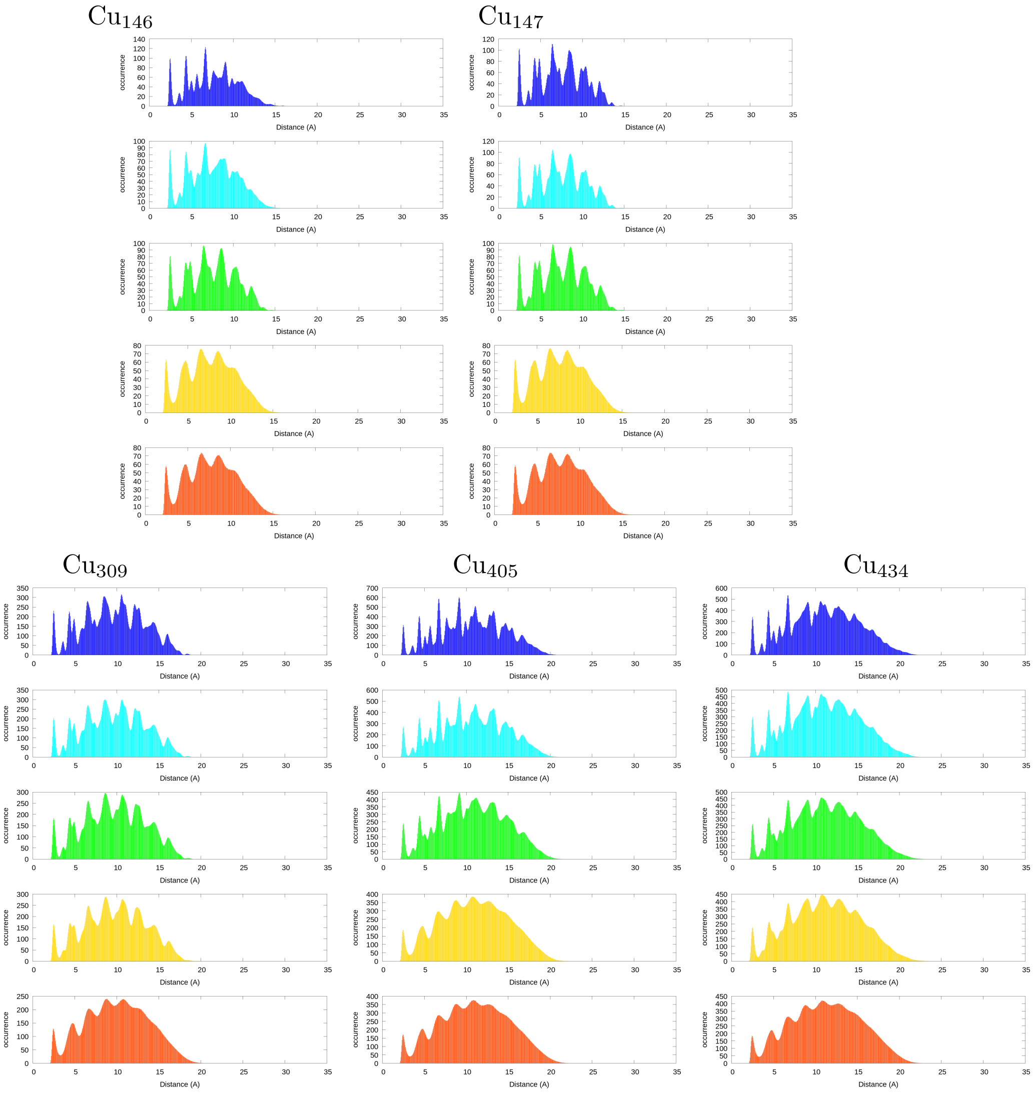

Figure S18: PDDF temperature evolution in Cu systems with size from 146 to 434 atoms. Temperature-color coding follows as blue = 450, cyan = 675, green = 800, yellow = 925, red = 1050.

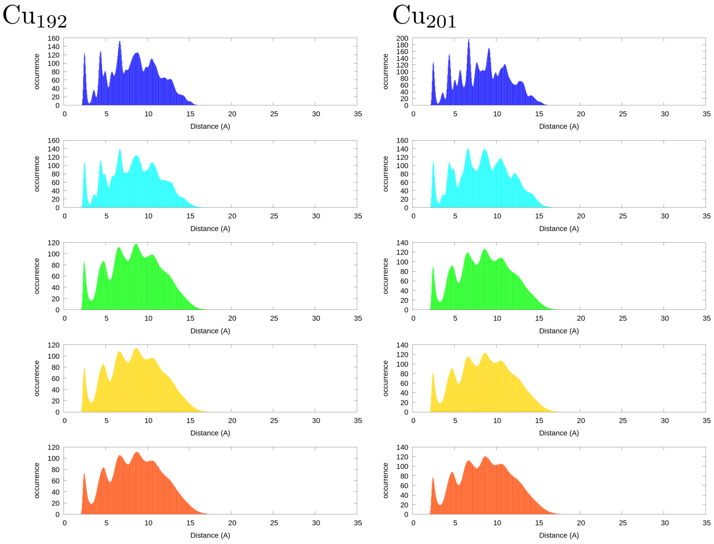

Cu_{192}

Cu_{201}

Figure S19: PDDF temperature evolution in Cu systems with size 192 and 201 atoms. Temperature-color coding follows as blue = 550, cyan = 775, green = 900, yellow = 1025, red = 1150.

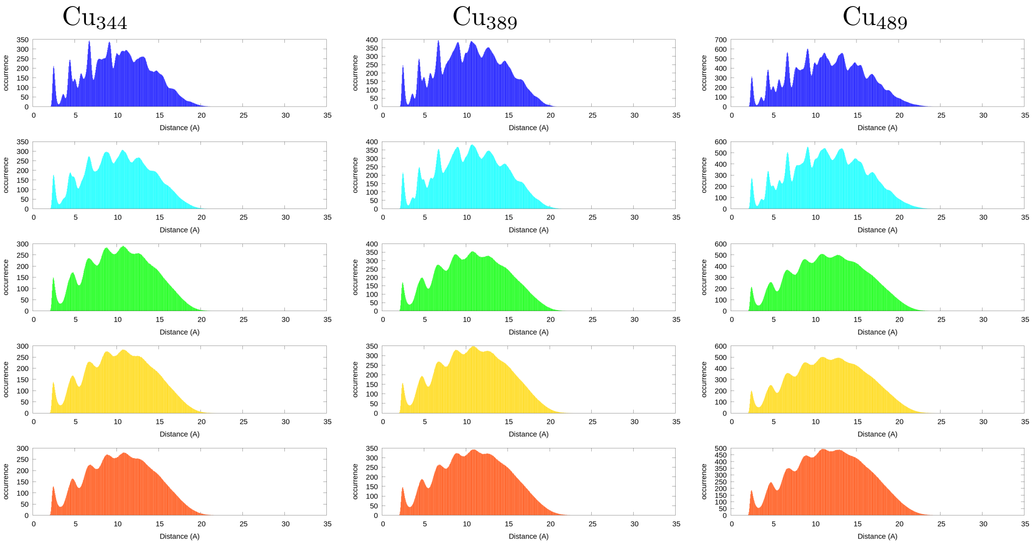

Figure S20: PDDF temperature evolution in Cu systems with size from 344, 389 and 489 atoms. Temperature-color coding follows as blue = 650, cyan = 875, green = 1000, yellow = 1125, red = 1150.

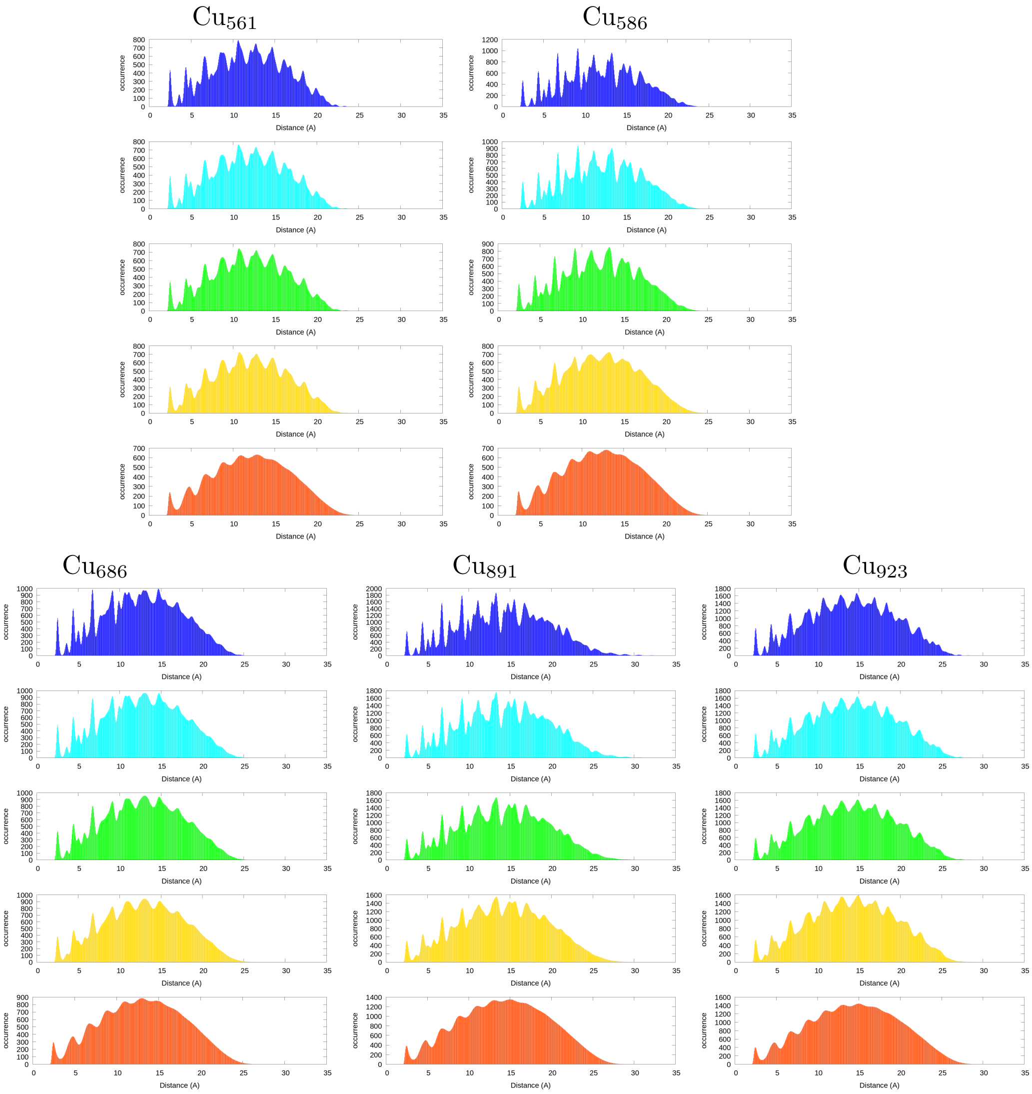

Cu_{561} Cu_{586} Cu_{686} Cu_{891} Cu_{923}

Figure S21: PDDF temperature evolution in Cu systems with size from 561 to 923 atoms. Temperature-color coding follows as blue = 450, cyan = 675, green = 800, yellow = 925, red = 1050.

S4.6 Palladium

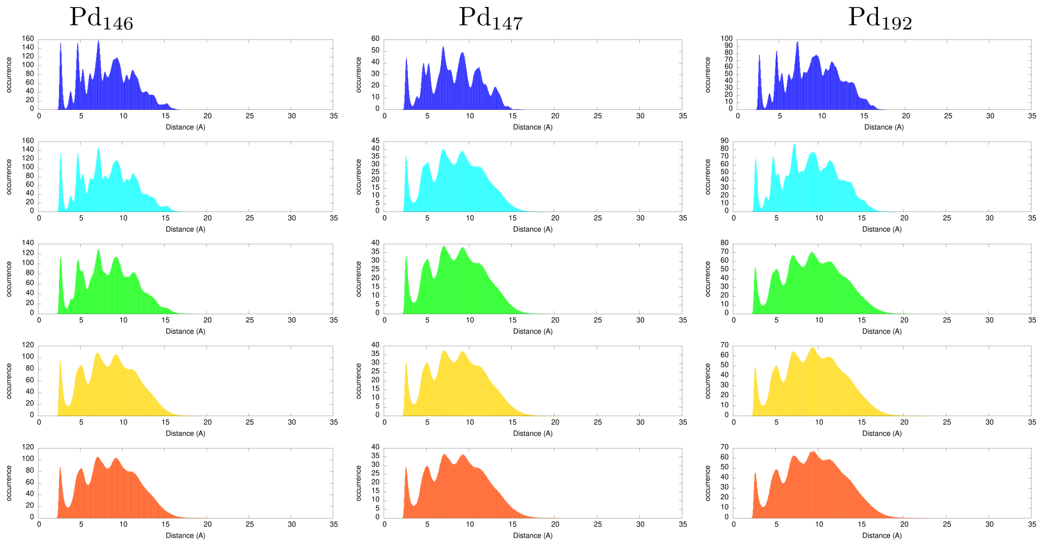
Pd_{146} Pd_{147} Pd_{192}

Figure S22: PDDF temperature evolution in Pd systems with size from 146 to 192 atoms. Temperature-color coding for size 146 follows blue = 525, cyan = 675, green = 800, yellow = 925, red = 1050. Size 147 follows blue = 725, cyan = 850, green = 975, yellow = 1075, red = 1175. Size 192 follows blue = 725, cyan = 850, green = 975, yellow = 1075, red = 1175.

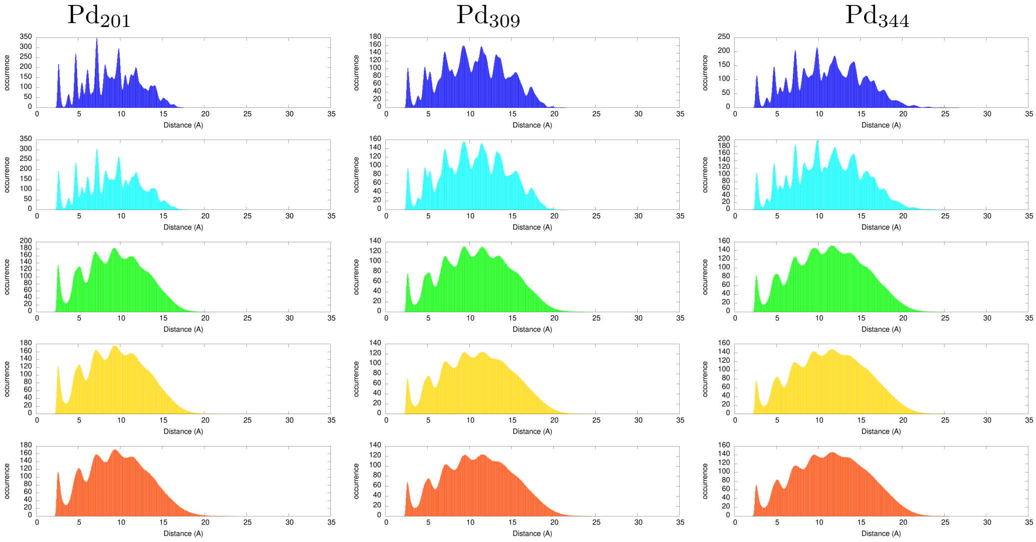

Figure S23: PDDF temperature evolution in Pd systems with size from 201 to 344 atoms. Temperature-color coding for size 201 follows blue = 525, cyan = 650, green = 900, yellow = 1050, red = 1175. Size 309 follows blue = 725, cyan = 800, green = 900, yellow = 1000, red = 1075. Size 344 follows blue = 725, cyan = 825, green = 950, yellow = 1075, red = 1200.

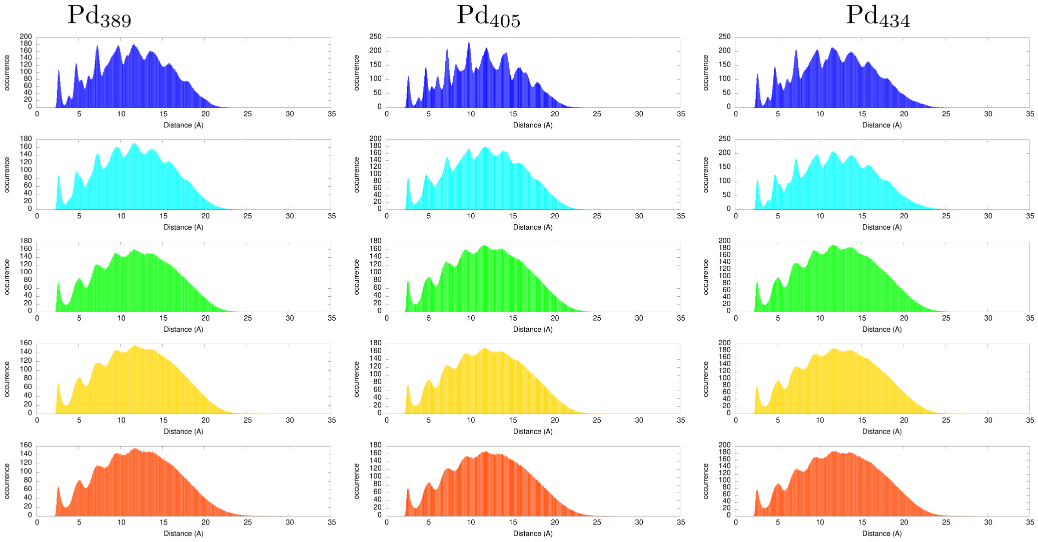

Figure S24: PDDF temperature evolution in Pd systems with size from 389 to 434 atoms. Temperature-color coding for size 389 follows blue = 825, cyan = 950, green = 1075, yellow = 1200, red = 1275. Sizes 405 and 434 follow blue = 825, cyan = 925, green = 1050, yellow = 1175, red = 1275.

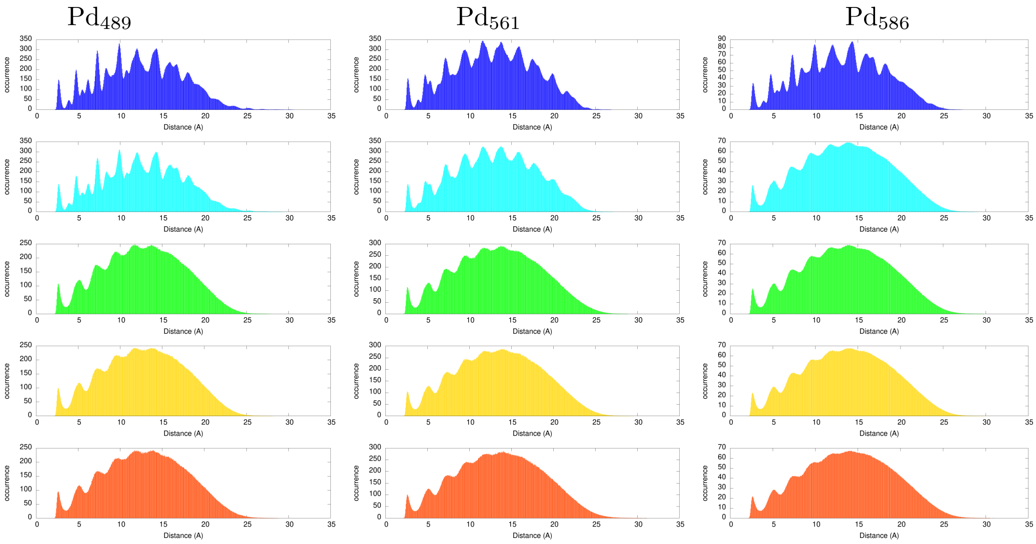

Figure S25: PDDF temperature evolution in Pd systems with size from 489 to 586 atoms. Temperature-color coding for size 489 follows blue = 925, cyan = 1025, green = 1125, yellow = 1325, red = 1575. Sizes 561 and 586 follow blue = 825, cyan = 925, green = 1025, yellow = 1175, red = 1300.

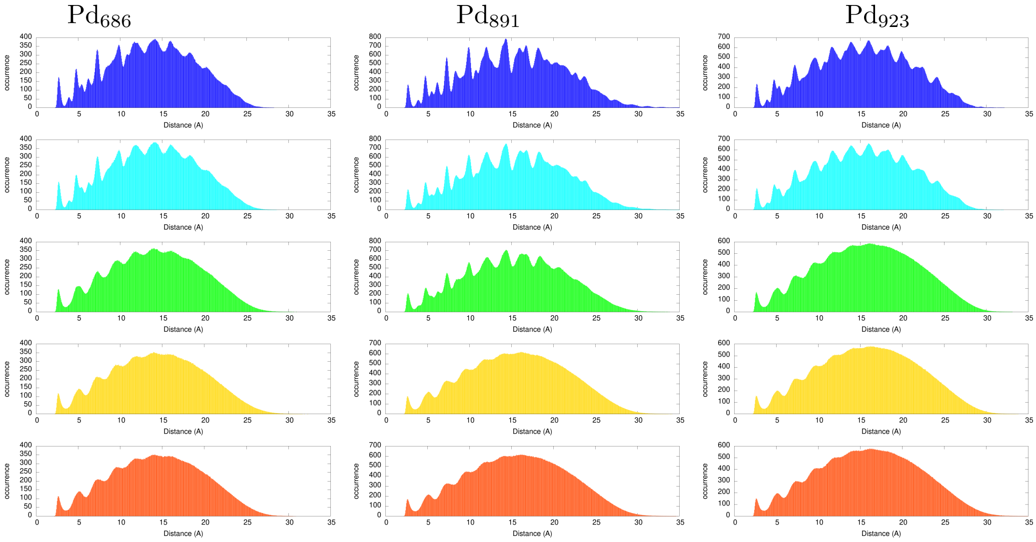

Figure S26: PDDF temperature evolution in Pd systems with size from 686 to 923 atoms. Temperature-color coding for size 686 follows blue = 825, cyan = 900, green = 1000, yellow = 1100, red = 1175. Size 891 follows blue = 825, cyan = 950, green = 1000, yellow = 1100, red = 1175. Size 923 follows blue = 1025, cyan = 1125, green = 1225, yellow = 1425, red = 1675.

S5 KL(h|c) dependence on the choice of the reference cold structure

In Figure S27 we report the comparison of the KL(h|c) temperature evolution with different choices of the reference cold structure, for the case of Pt clusters of 201 atoms with an initial truncated octahedral morphology. Note the decrease in the values observed for KL(h|c) when the cold reference is taken at higher temperatures and the absence of a quasi first order transition for the case of cold reference configurations taken after the melting (melting temperature is 1125K).

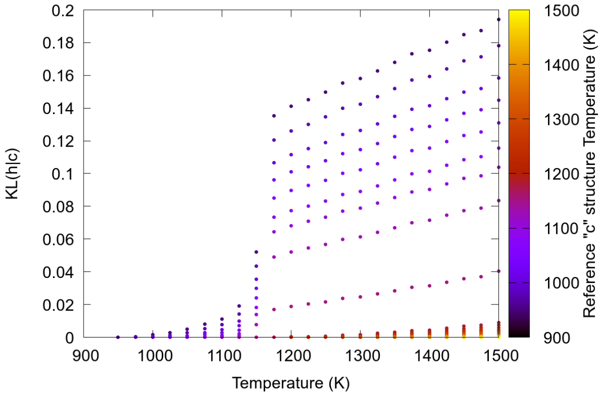

Figure S27: Pt 201 nanoparticle KL(h|c) temperature dependent evolution for the choice of different color-coded initial reference structures.

S6 KL(h|c) dependence on the choice of the PDDF bin width

In figure S28 we report the comparison of the KL(h|c) temperature evolution for different choices of the bin width at which the pair distance distribution function of the nanoparticle is discretized. Data for a Pt nanoparticle of 201 atoms are reported. In agreement with what predicted from Figure S2, with a distance bin width larger than 0.05 Å this analysis does not provide information about the melting transition.

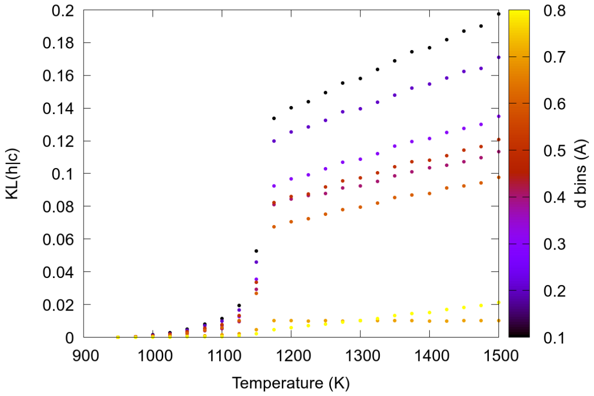

Figure S28: Pt 201 nanoparticle KL(h|c) temperature dependent evolution for the choice of 10 PDDF binning width.

S7 KL(h|c) and structural rearrangements, the case of pre-melting transitions in slowly heated Cu nanoparticles

In this section we discuss results on the behaviour of the KL(h|c) temperature evolution in a system undergoing solid-solid structural rearrangements during a small heating rate temperature ramp.

While PDDF peaks at distances above the bulk lattice parameter correspond to peculiar structural features in the nanoparticle such as the presence of grain-boundaries and 5-fold symmetry axis, first and second nearest neighbour peaks are only partially affected by solid-solid rearrangements. Although the process can lead the nanoparticle to assume an increased or decreased average coordination, peaks at the first and second nearest neighbours characteristic distances are essentially fixed by size (albeit their occurrence can vary). Consequently the KL(h|c) of the PDDF taken up to the second peak is not sensitive to both minor and major solid-solid rearrangements. This result should be held into account during the search of, e.g. collective variables for enhanced sampling techniques. However an in depth discussion of this finding is beyond the scope of this article.

Let us discuss the case of a Cu nanoparticle of 146 atoms with an initial Oh structure, undergoing a structural rearrangement towards an Ih morphology. Figure S29 reports in the top two panels the different trends found for the KL(h|c), if it is calculated for the full (top) pair distance distribution function of the nanoparticle, or up to the second nearest neighbour distance (middle panel). In both panels we overlay the evolution of the Excess Energy with respect to Temperature in red.

In the third panel we report the evolution of three common nearest neighbour analysis (CNA) [J. Phys. Chem. 1987, 91, 19, 4950–4963] signature during each one of the eight independent simulations considered. CNA characterizes nearest neighbours as a function of the connectivity network of their shared neighbours. Let i and j be a pair of atoms, they are defined as nearest neighbours if their distance is shorter than a cut-off (1.2 times the bulk nearest neighbour distance in this study).

Following the CNA analysis they will be assigned a three integers signature (r, s, t). r is the number of the common nearest neighbours of the pair. s is the number of bonds between them (the r atoms). t is the length of longest chain among the r atoms. A pair is in a face centred cubic environment if it presents a (4,2,1) signature, along a 5-fold symmetry axis if it is assigned a (5,5,5) signature, and along a grain boundary if their CNA signature is (4,2,2).

At a temperature close to 600K we consistently observe a sharp increase in the number of (5,5,5) and (4,2,2) signatures, paralleled by a decrease in the number of atoms in FCC arrangement (i.e. (4,2,1) signature). This change in the CNA distribution corresponds to the structural rearrangement of the initial Octahedral nanoparticle, undergoing a solid-solid transition towards an Icosahedron.

Before this solid-solid rearrangement we note that atomic rearrangements leading to a defected FCC morphology occur in relatively numerous occasions. These correspond to an increase of (4,2,2) signature occurrences at the expense of neighbour pairs characterized by a (4,2,1) signature.

If the full PDDF is taken into account during the KL(h|c) analysis, a peak is observed preceding the full transition towards the icosahedron. This is not the case for a KL(h|c) PDDF analysis limited to the bulk lattice parameter. As shown by the change in excess energy with the increase of temperature (middle panel), the transition takes place at 780 K, close to the melting temperatures found with a Molecular Dynamics protocol employing a 5 times faster heating rate. Indeed, the KL(h|c) PDDF analysis limited to the bulk lattice parameter displays a sharp increase at this temperature. The melting transition is also signalled by the strong change in the CNA signatures, around 775 K.

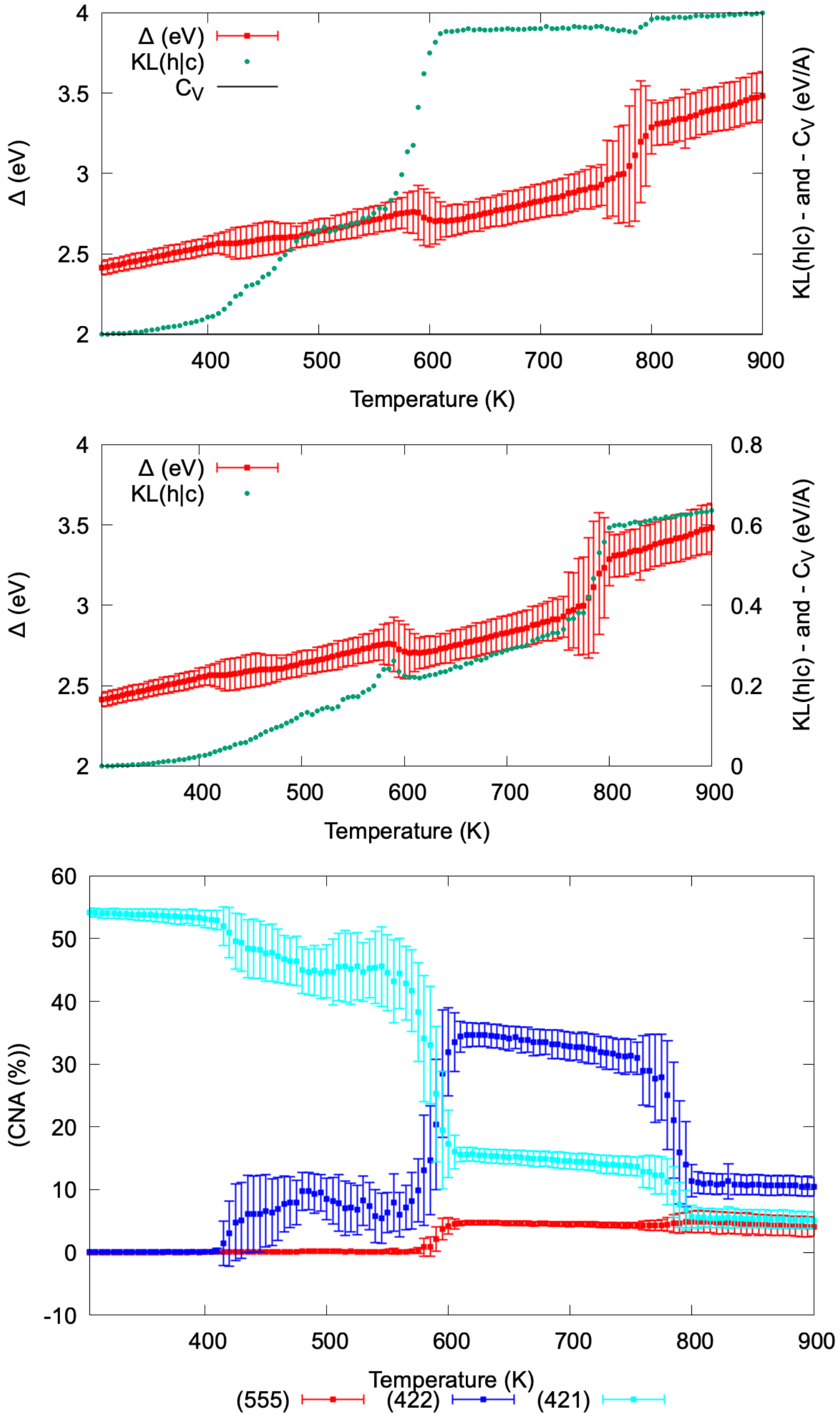

Figure S29: The temperature evolution of the KL(h|c) of the whole PDDF (green) or limited to the bulk lattice parameter distance (blue) of a 146 atoms Cu cluster with an initial Oh morphology. A solid-solid transition takes place at 650K, liquid-solid phase change happens at 800K. The extended KL(h|c) measure is more affected by the solid-solid rather than the solid-liquid change. CNA signatures relative occurrence is also reported in red (5,5,5), blue (4,2,2), and cyan (4,2,1).

S8 KL vs temperature - Energy vs temperature

In this subsection we report the caloric curves overlaid with the KL (h|c) vs temperature curves. Note the correspondence of phase change in the two curves.

S8.1 Platinum

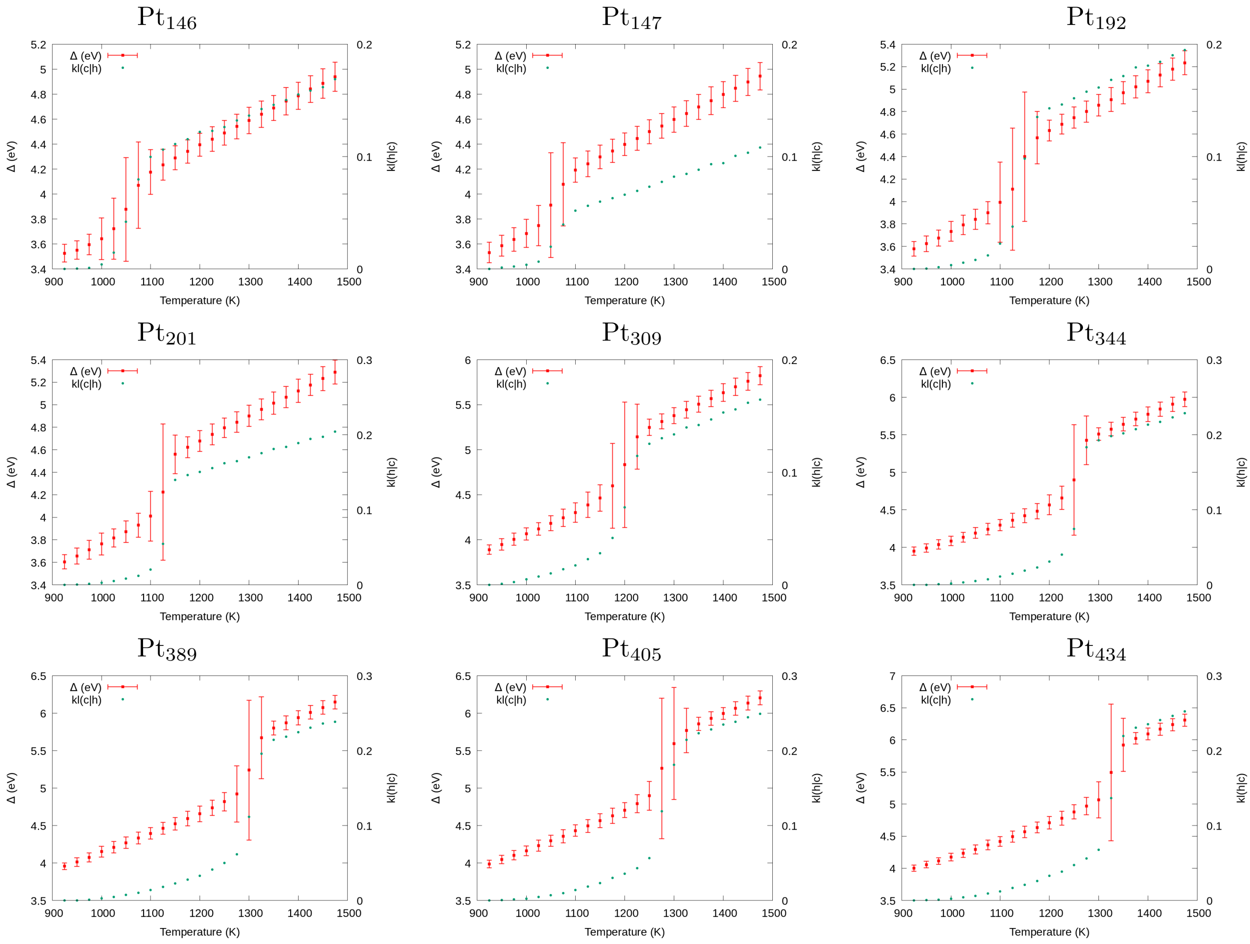

Figure S30: excess energy and KL (h|c) temperature evolution in Pt systems with size from 146 to 405 atoms

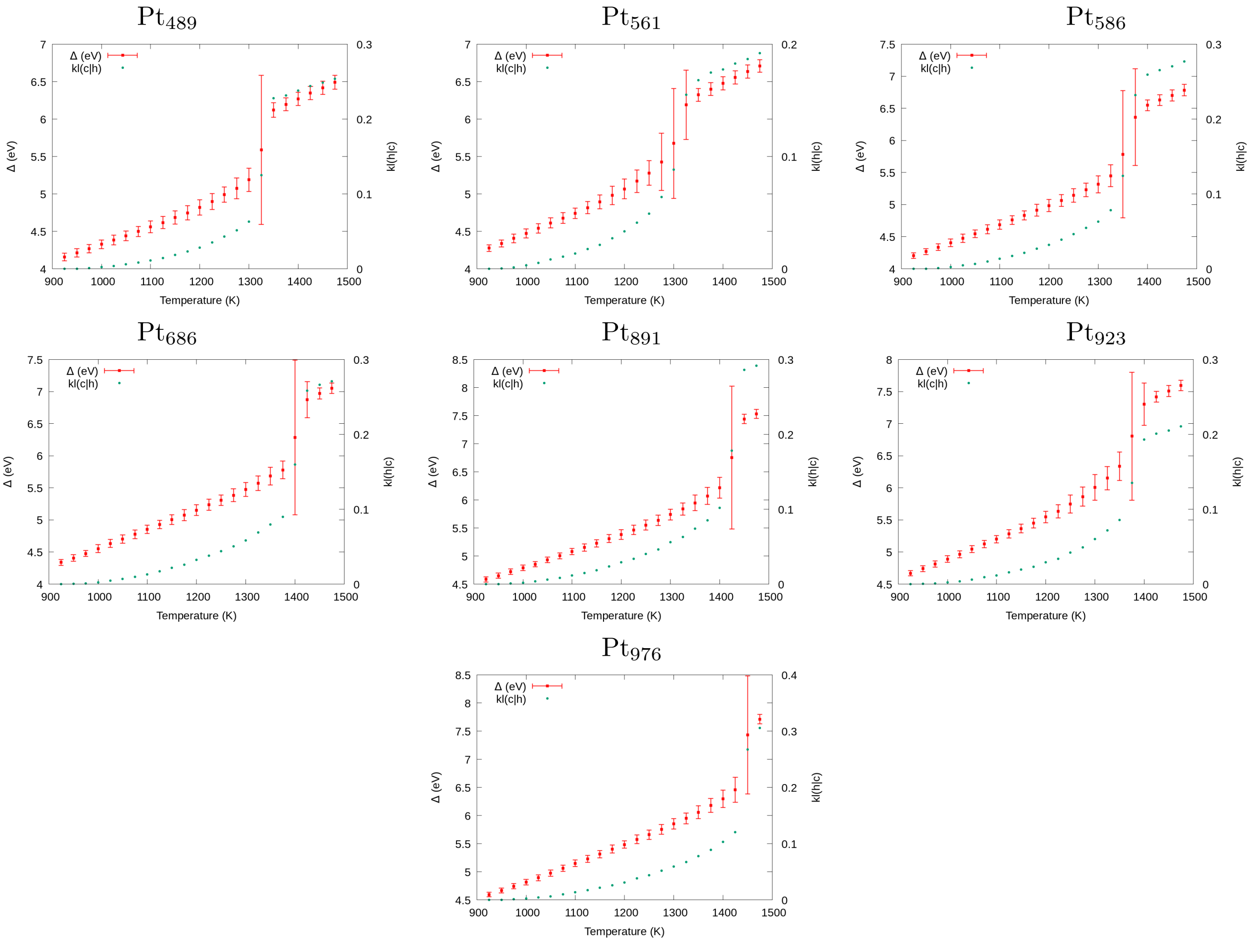

Figure S31: PDF temperature evolution in Pt systems with size from 434 to 976 atoms

S8.2 Gold

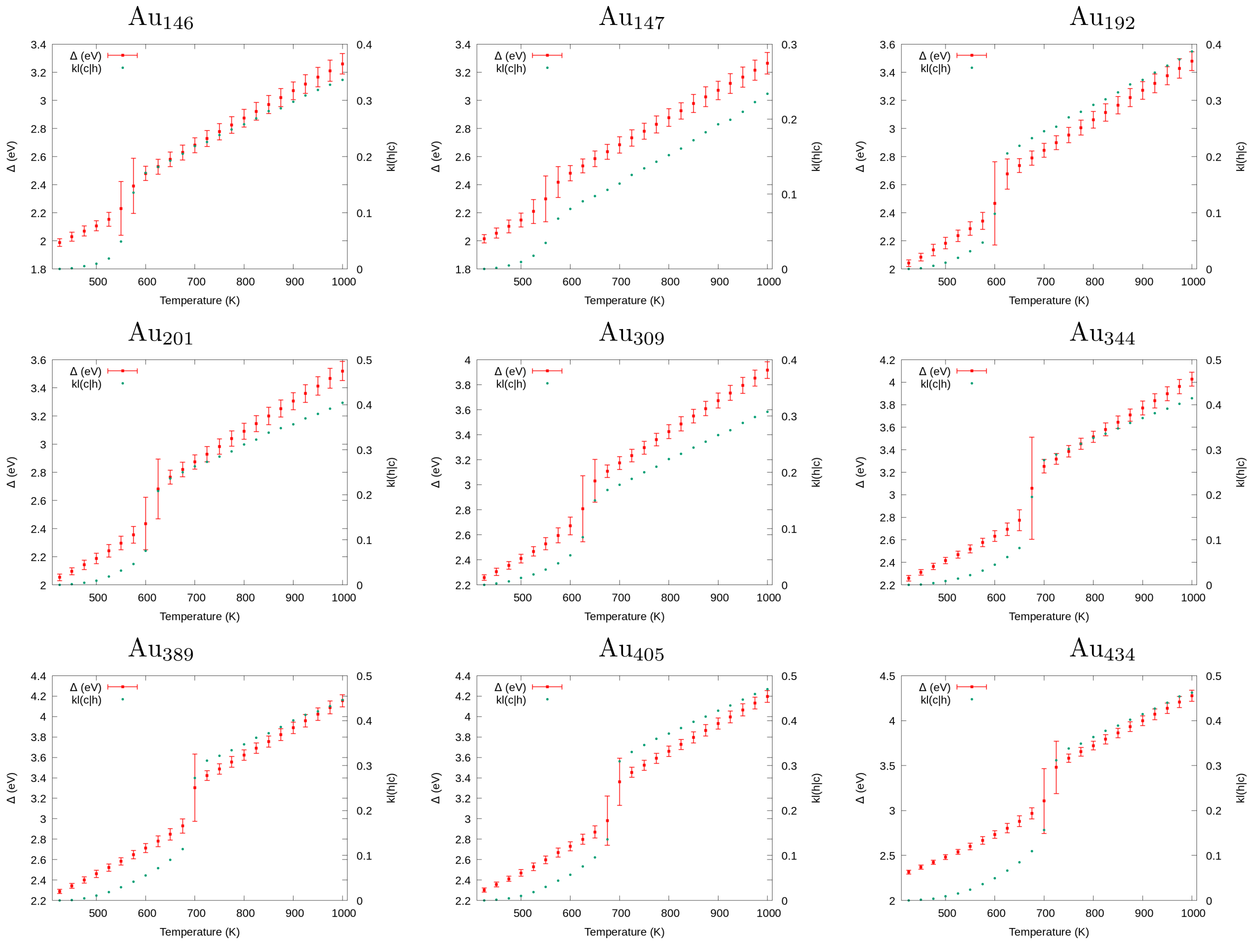

Figure S32: excess energy and KL (h|c) temperature evolution in Au systems with size from 146 to 405 atoms

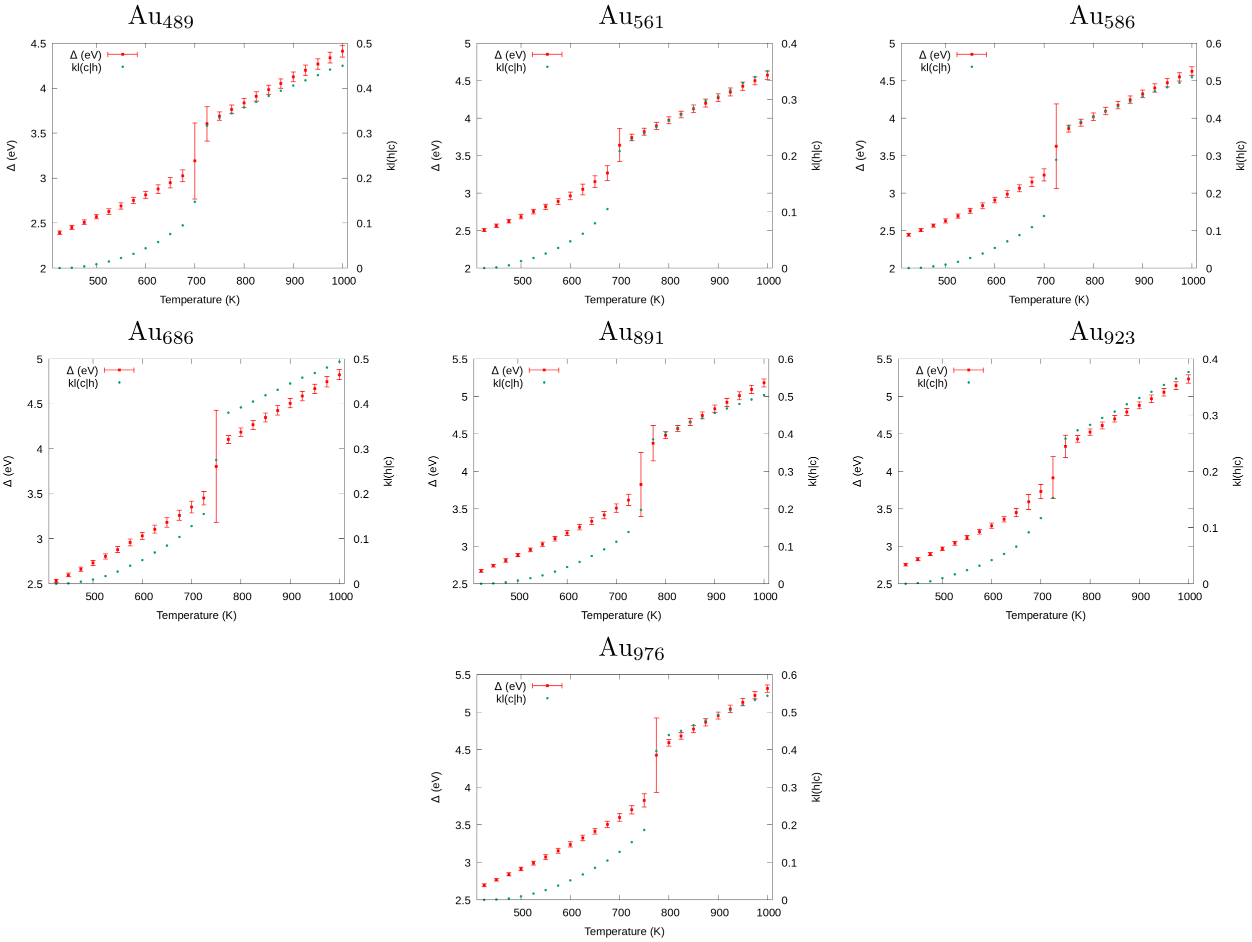

Figure S33: PDF temperature evolution in Au systems with size from 434 to 976 atoms

S8.3 Silver

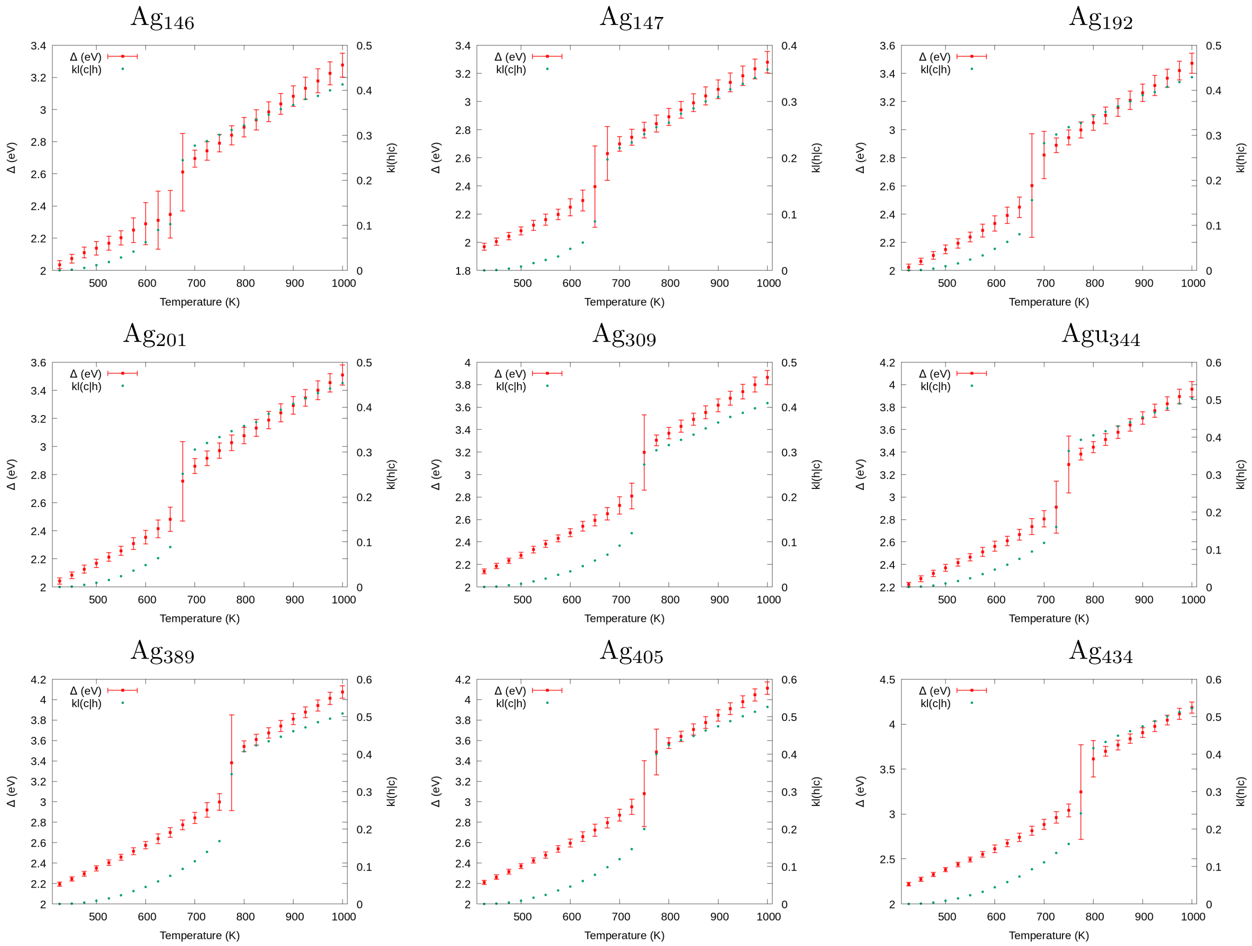

Figure S34: excess energy and KL (h|c) temperature evolution in Ag systems with size from 146 to 405 atoms

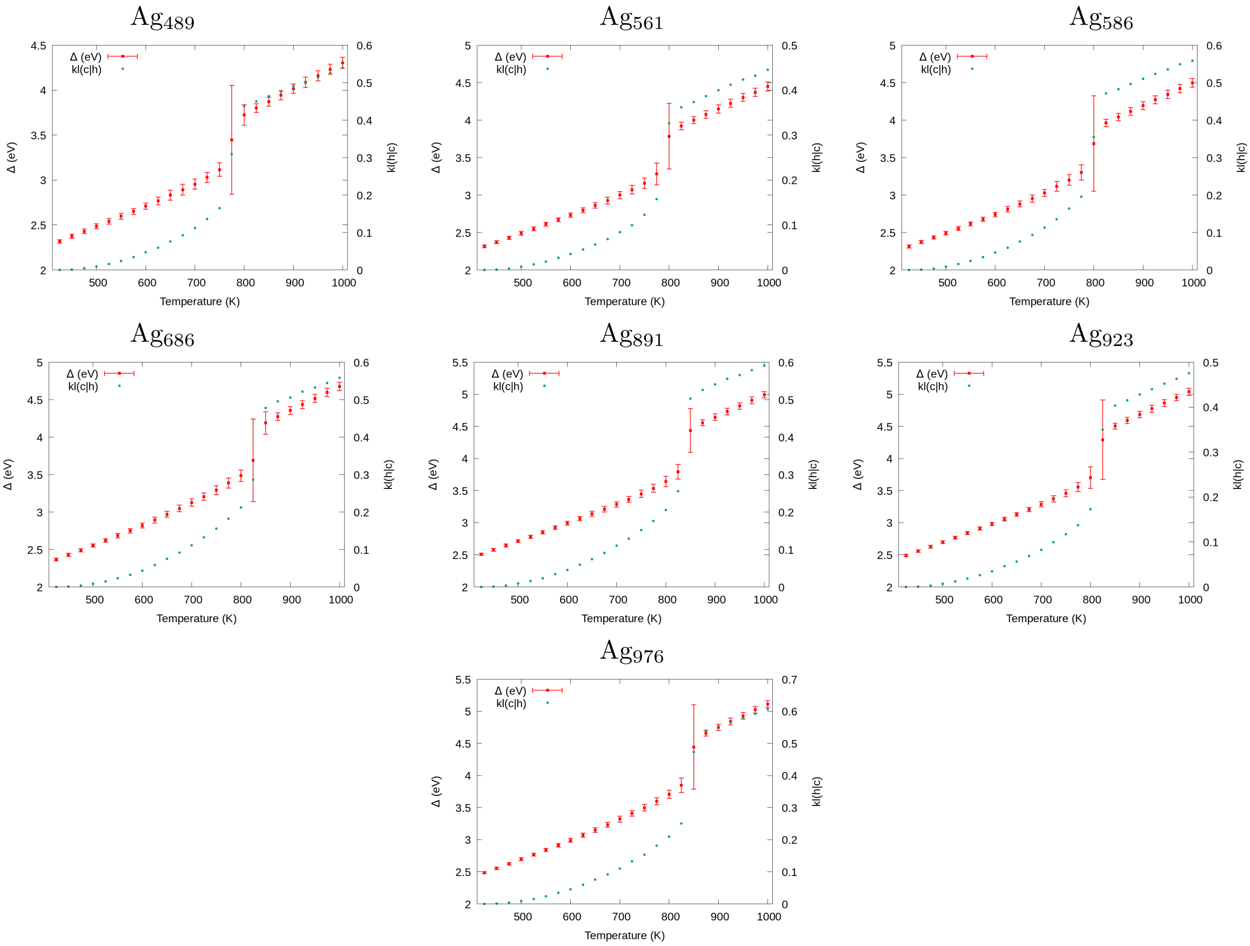

Figure S35: PDF temperature evolution in Ag systems with size from 434 to 976 atoms

S8.4 Nickel

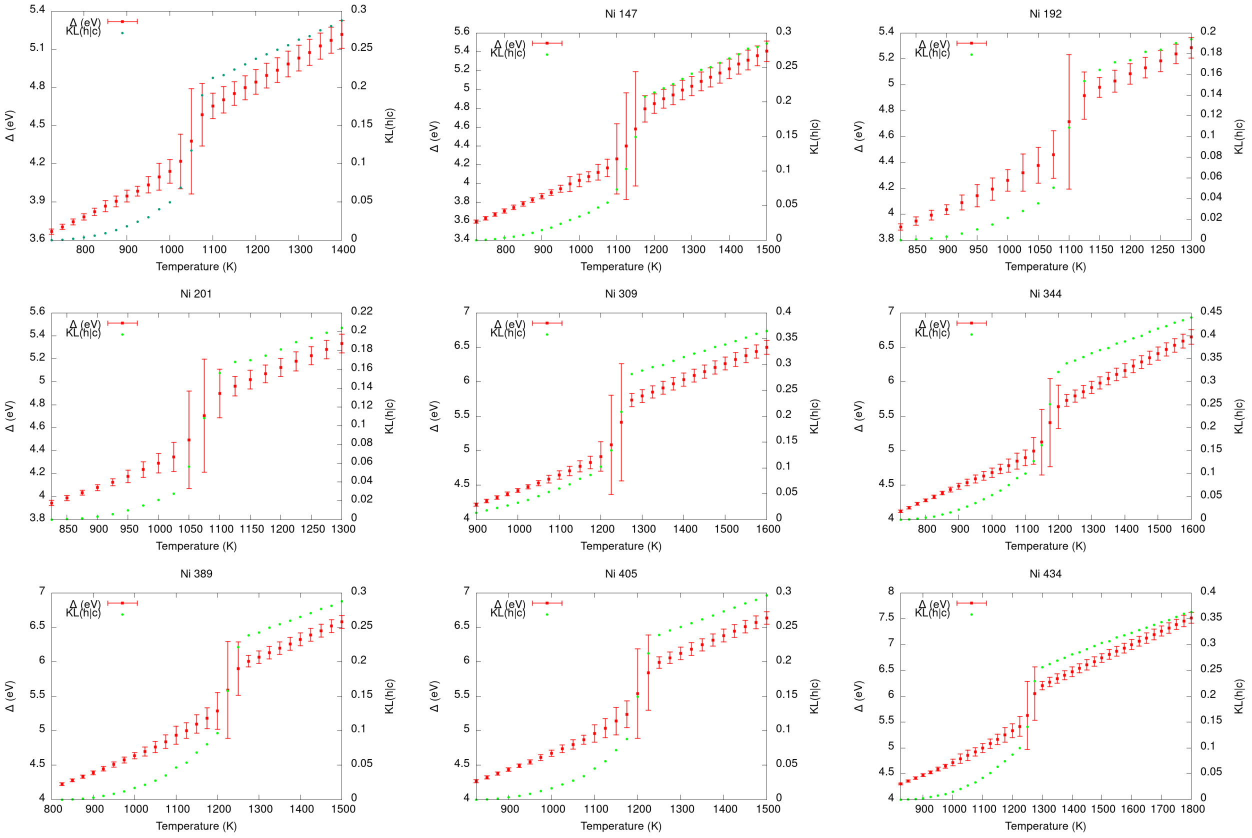

Figure S36: excess energy and KL (h|c) temperature evolution in Ni systems with size from 146 to 405 atoms

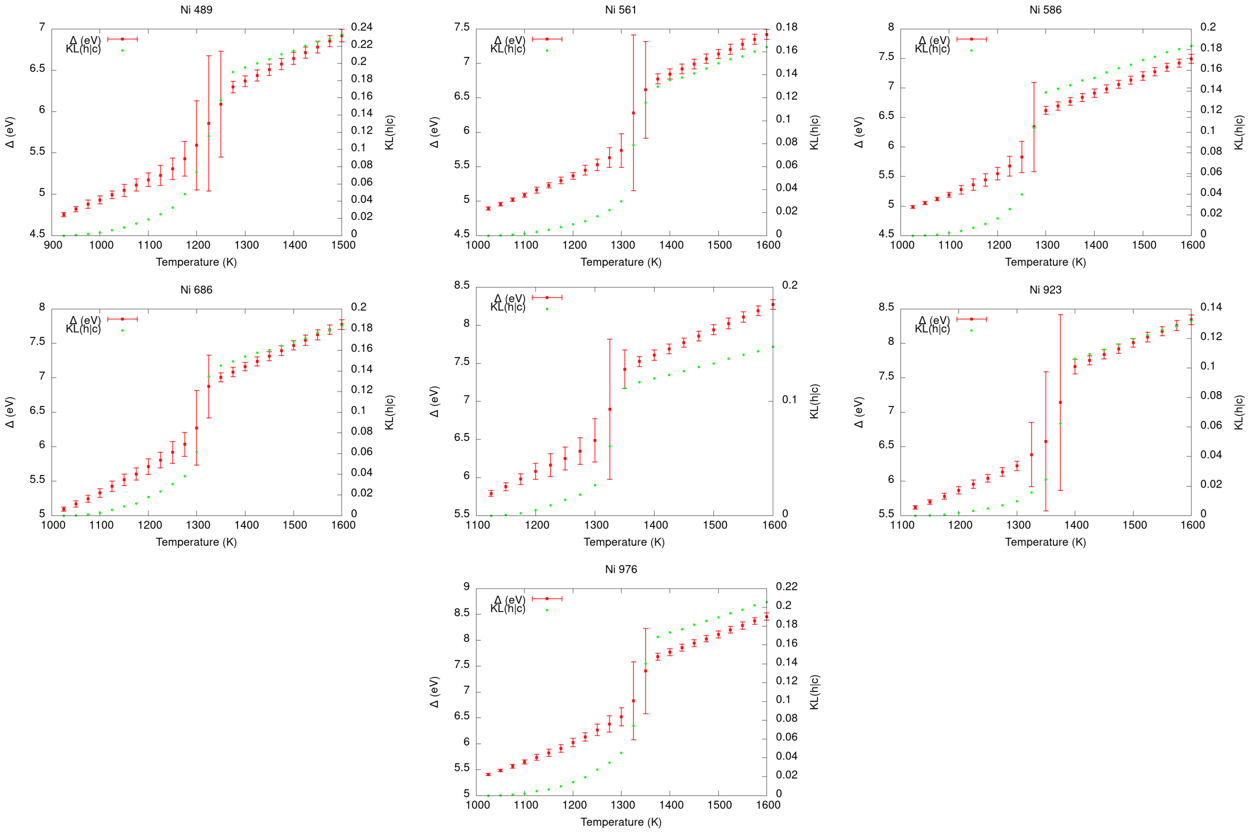

Figure S37: PDF temperature evolution in Ni systems with size from 434 to 976 atoms

S8.5 Copper

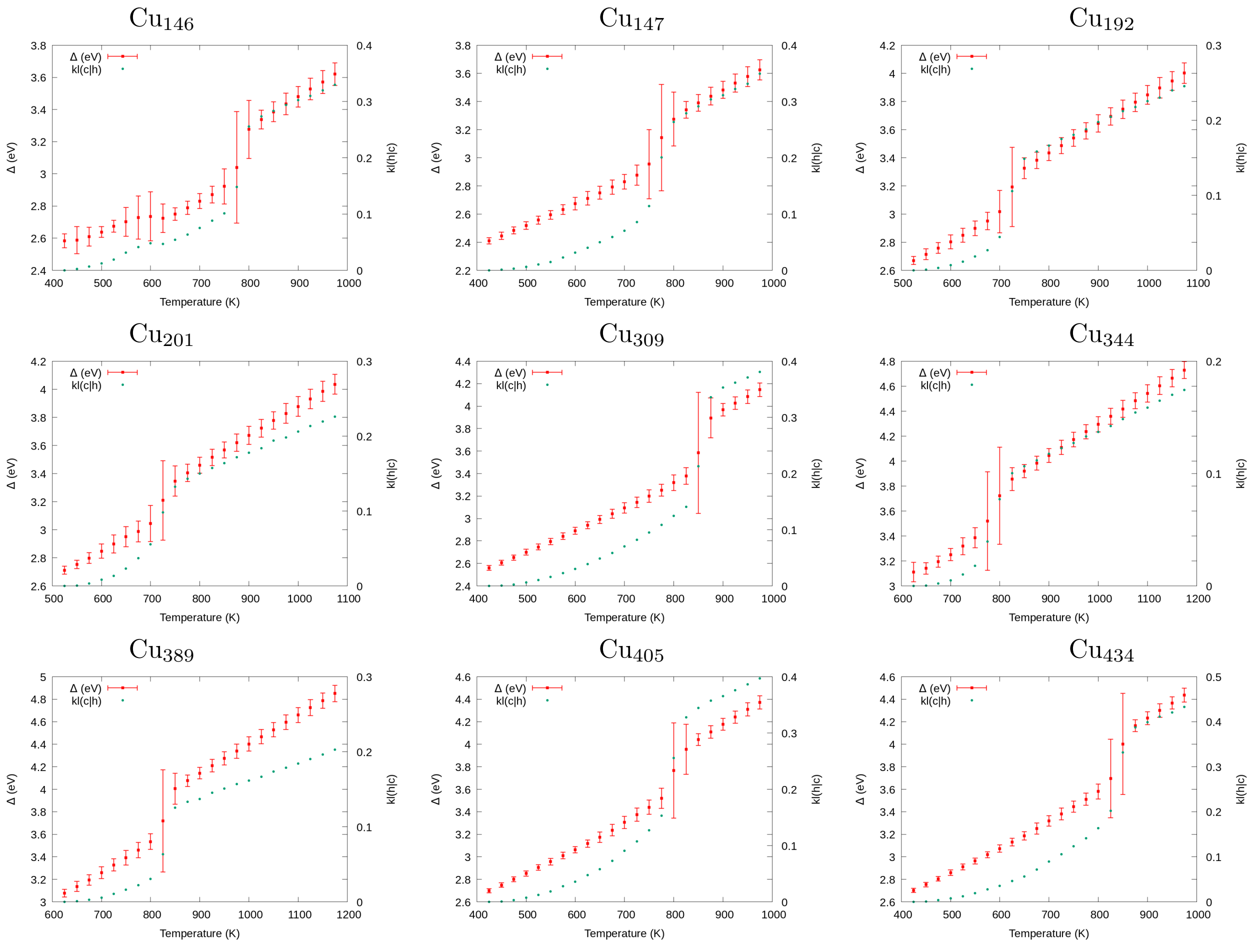

Figure S38: excess energy and KL (h|c) temperature evolution in Cu systems with size from 146 to 405 atoms

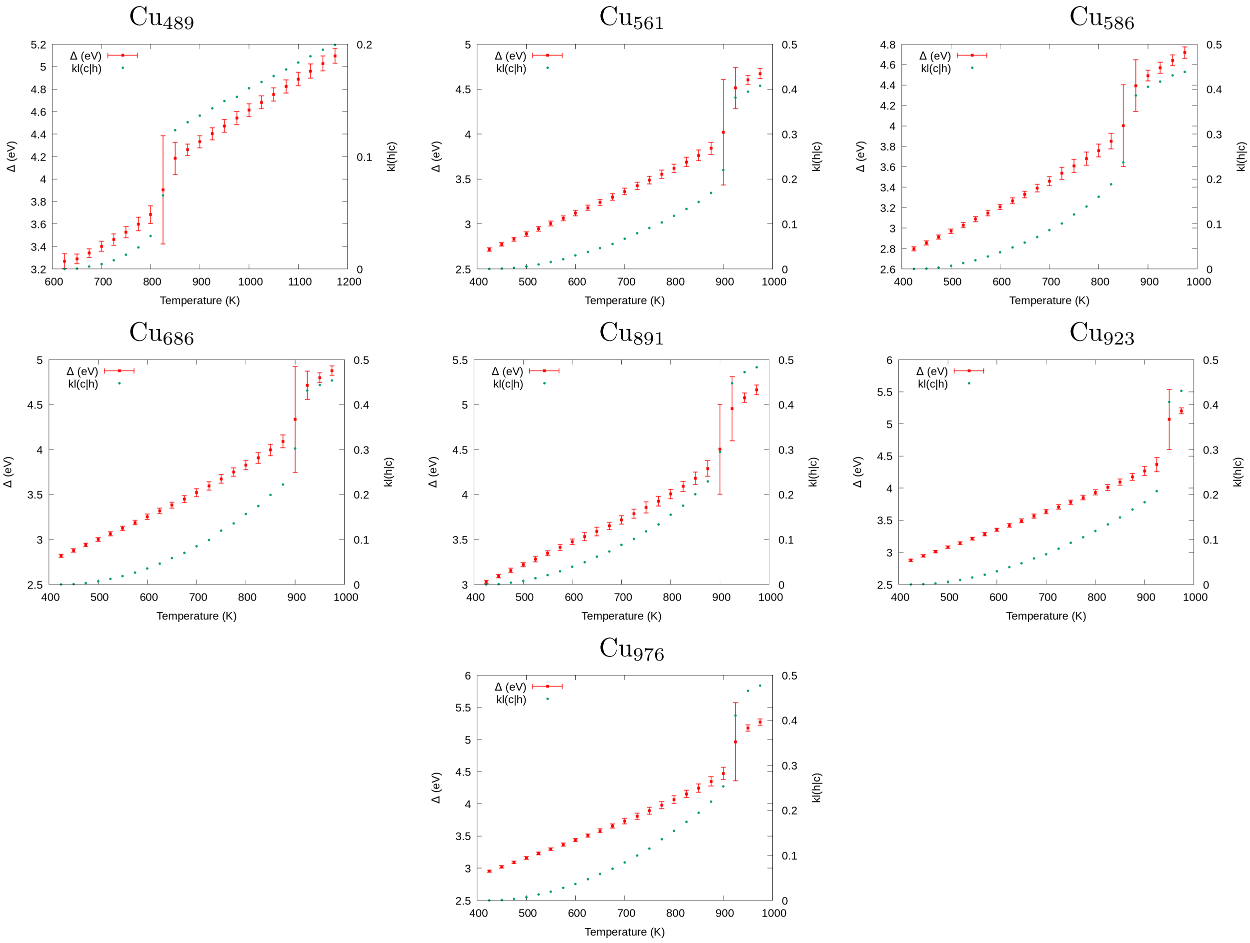

Figure S39: PDF temperature evolution in Cu systems with size from 434 to 976 atoms

S8.6 Palladium

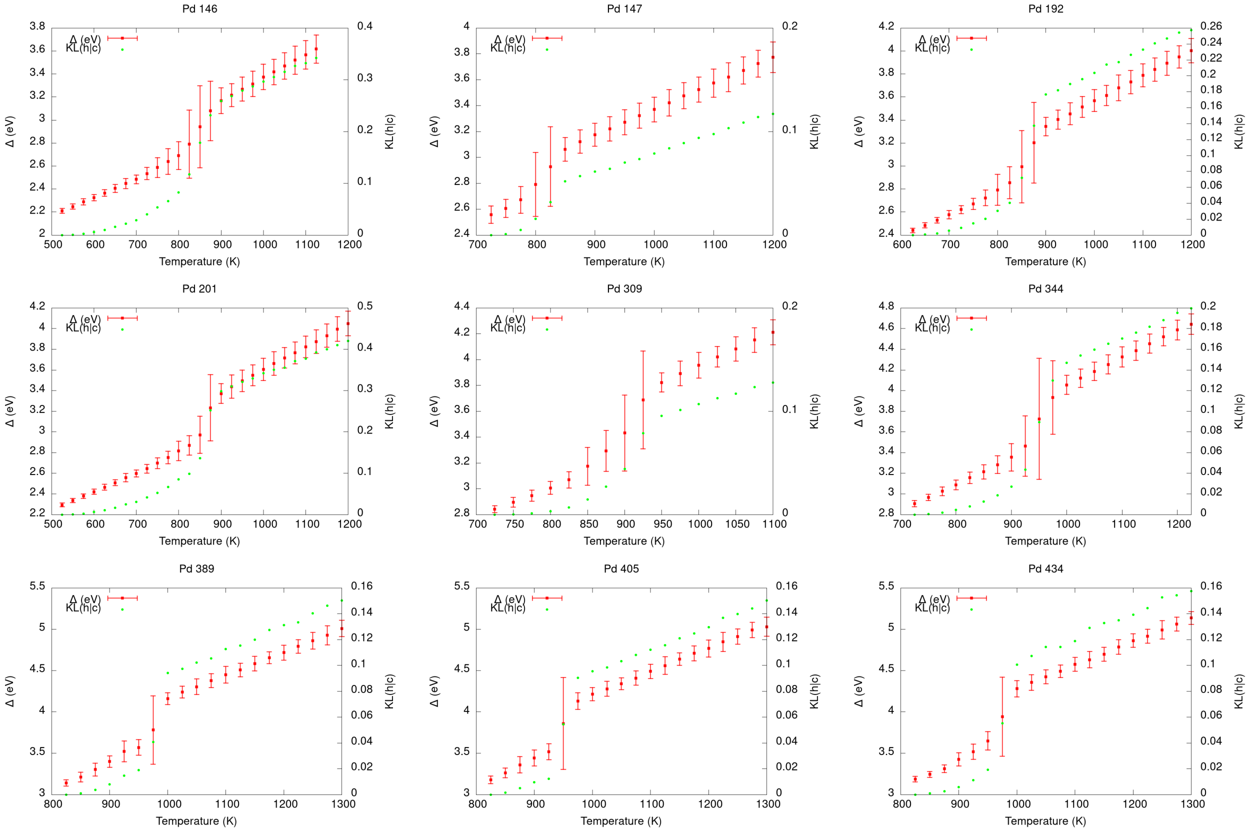

Figure S40: excess energy and KL (h|c) temperature evolution in Pd systems with size from 146 to 405 atoms

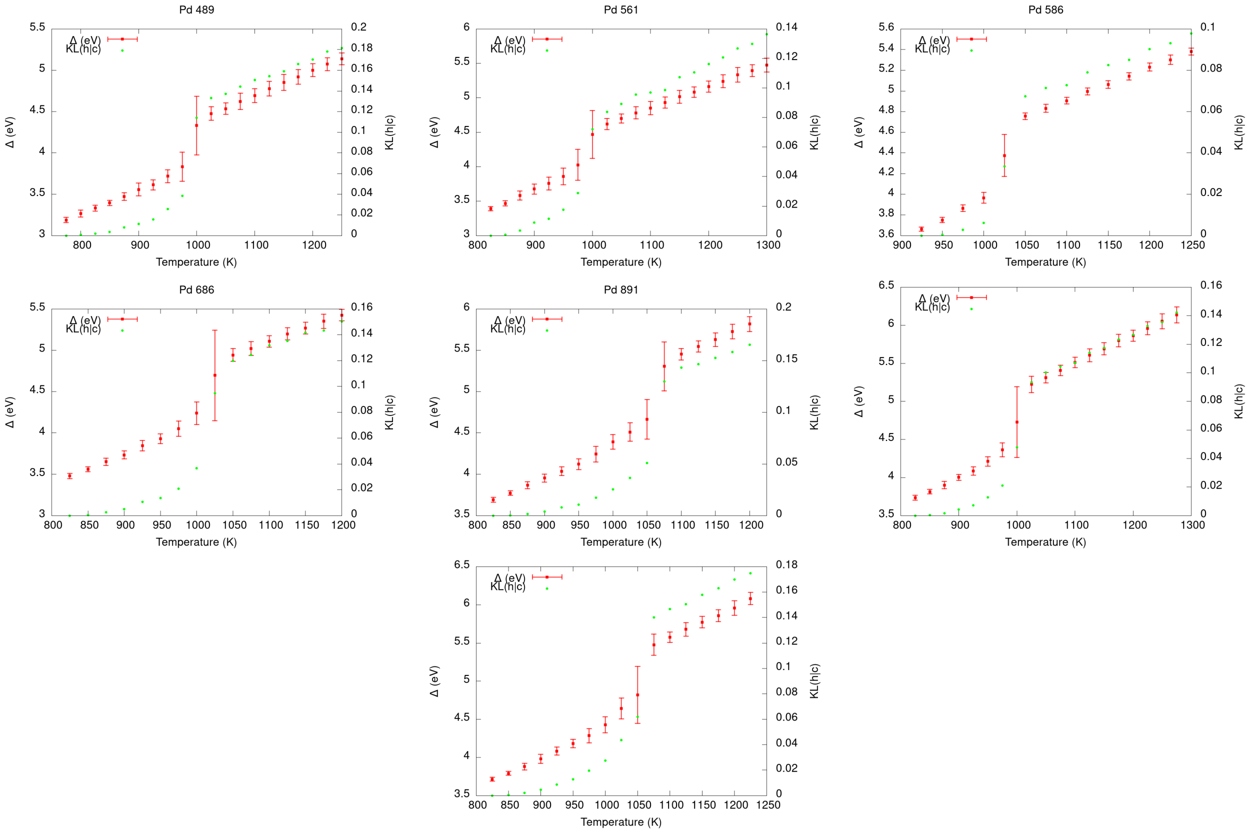

Figure S41: PDF temperature evolution in Pd systems with size from 434 to 976 atoms

S9 Recap Table

In Table S1 we report the melting temperatures found by looking at the caloric curve and the KL vs temperature evolution, as per detailed in the main manuscript.

						$T_{melting}$							
		Ag		Au		Cu		Ni		Pd		Pt	
Shape	N of atoms	caloric	KL(H|c)	caloric	KL(H|c)	caloric	KL(H|c)	caloric	KL(H|c)	caloric	KL(H|c)	caloric	KL(H|c)
Oh	146	675	675	550	550	775	775	1050	1050	850	850	1050	1050
Ih	147	650	650	550	550	775	775	1125	1125	825	825	1050	1050
MDh	192	675	675	600	600	725	725	1100	1100	850	850	1150	1150
TOh	201	675	675	600	600	725	725	1050	1050	875	875	1125	1125
Ih	309	775	775	625	625	850	850	1225	1225	925	925	1200	1200
Oh	344	725	725	675	675	775	775	1150	1150	950	950	1250	1250
MDh	389	775	775	700	700	825	825	1225	1225	975	975	1300	1300
TOh	405	750	750	675	675	800	800	1200	1200	950	950	1275	1275
MDh	434	775	775	700	700	850	850	1250	1250	975	975	1325	1325
Oh	489	775	775	700	700	825	825	1225	1225	1000	1000	1325	1325
Ih	561	800	800	700	700	900	900	1325	1325	1000	1000	1300	1300
TOh	586	800	800	725	725	850	850	1275	1275	1025	1025	1350	1350
MDh	686	825	825	750	750	900	900	1300	1300	1025	1025	1400	1400
Oh	891	850	850	750	750	900	900	1325	1325	1075	1075	1425	1425
Ih	923	825	825	725	725	950	950	1375	1375	1000	1000	1375	1375
TOh	976	850	850	775	775	925	925	1325	1325	1050	1050	1450	1450

Table S1: Summary of the melting temperatures ($T_{melting}$ - in K) estimated for nanoparticles of different shapes (first column), number of atoms (second column), and composition (first row), by monitoring the excess energy or the KL(h|c) evolution. For the case of the excess energy curves we define the melting temperature as the one with the largest standard deviation. For the KL(h|c) curves we instead define the melting temperature as the one where the KL(h|c) value is the most different from the preceding and subsequent temperature. Note the perfect match between the two estimates. Error bars are taken as the Δ T factor determining the increase of temperature at each iteration of the iterative temperature MD simulations, 25K.

S10 Environment effect

In this subsection we report the caloric curves overlaid with the KL (h|c) vs temperature curves for the case of 201 atoms NPs in a strongly interacting implicit environment (see Section II A in the main manuscript for additional details on how the latter is modelled).

Note how the system phase change temperature is systematically shifted to colder temperatures in all the systems under consideration, for an increasingly strong interaction with the implicit environment. Similarly we consistently observe larger standard deviations in the excess energy.

S10.1 Platinum

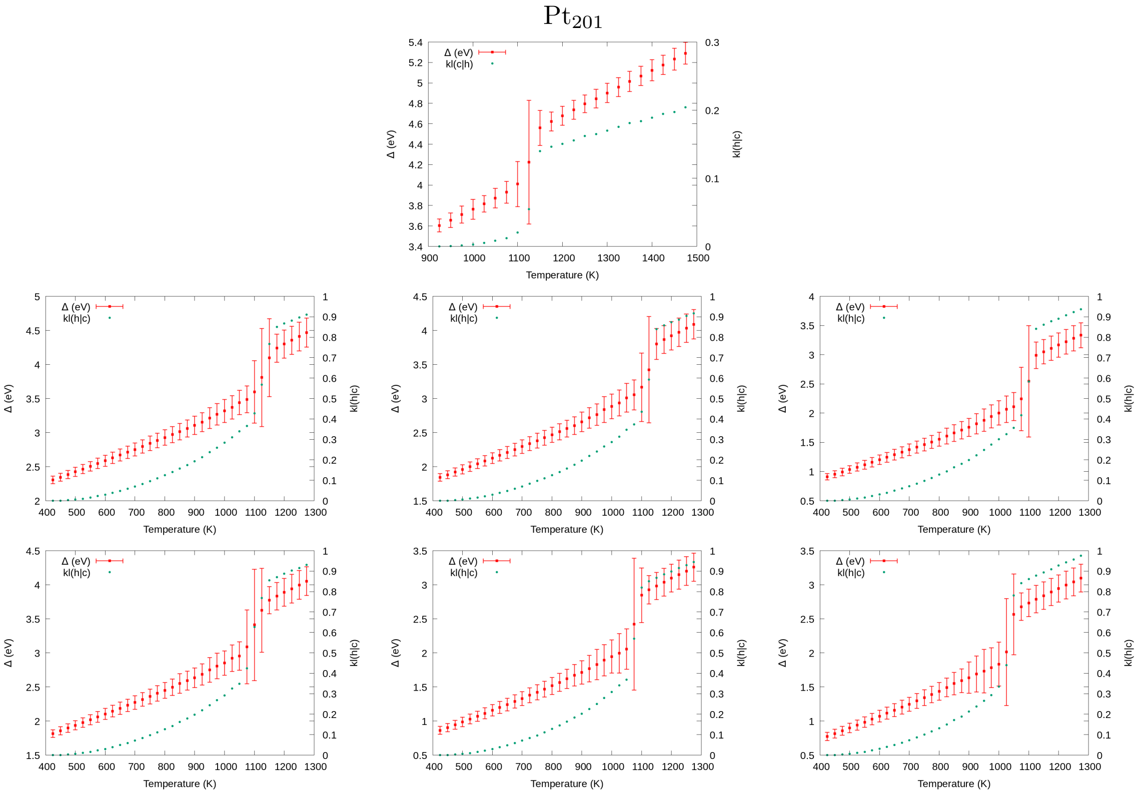

Figure S42: Excess energy and KL (h|c) temperature evolution in Pt systems with size 201 atoms in environments with different interaction strength and nature. The top central figure is Pt_{201} without environment, shown as reference. The phase change shifts towards colder temperatures with an increasing interaction.

S10.2 Palladium

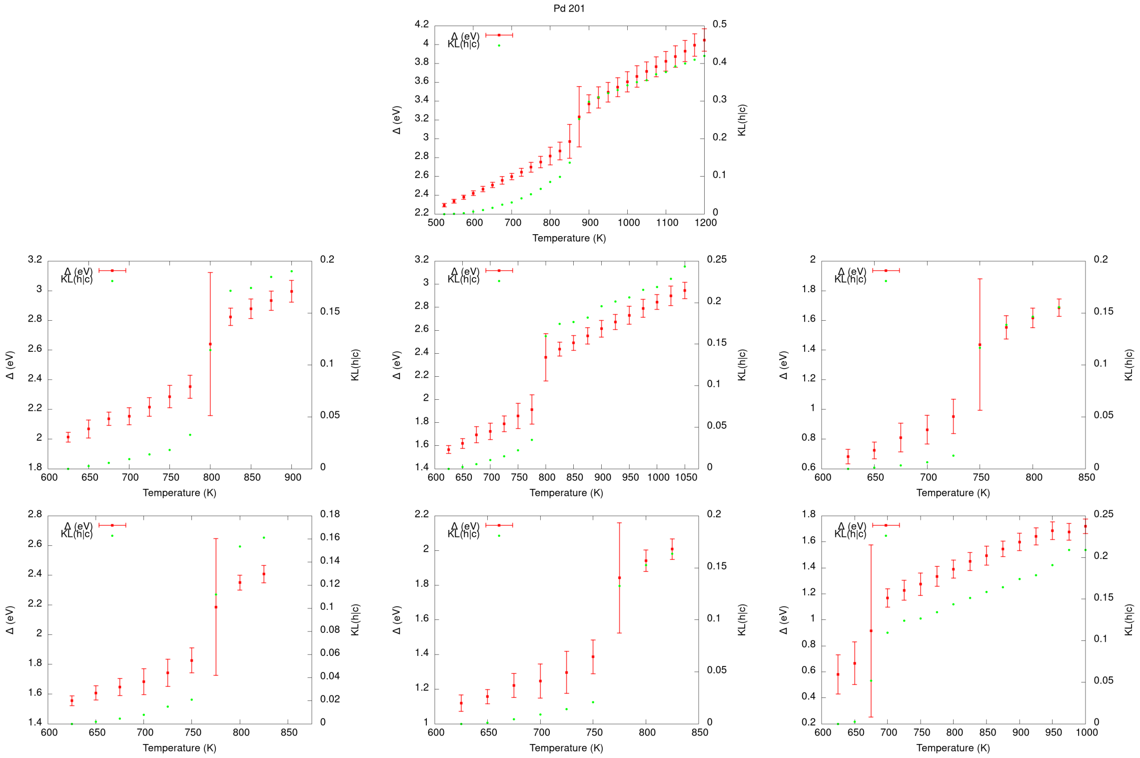

Figure S43: Excess energy and KL (h|c) temperature evolution in Pd systems with size 201 atoms in environments with different interaction strength and nature. The top central figure is Pd_{201} without environment, shown as reference. The phase change shifts towards colder temperatures with an increasing interaction.

S10.3 Nickel

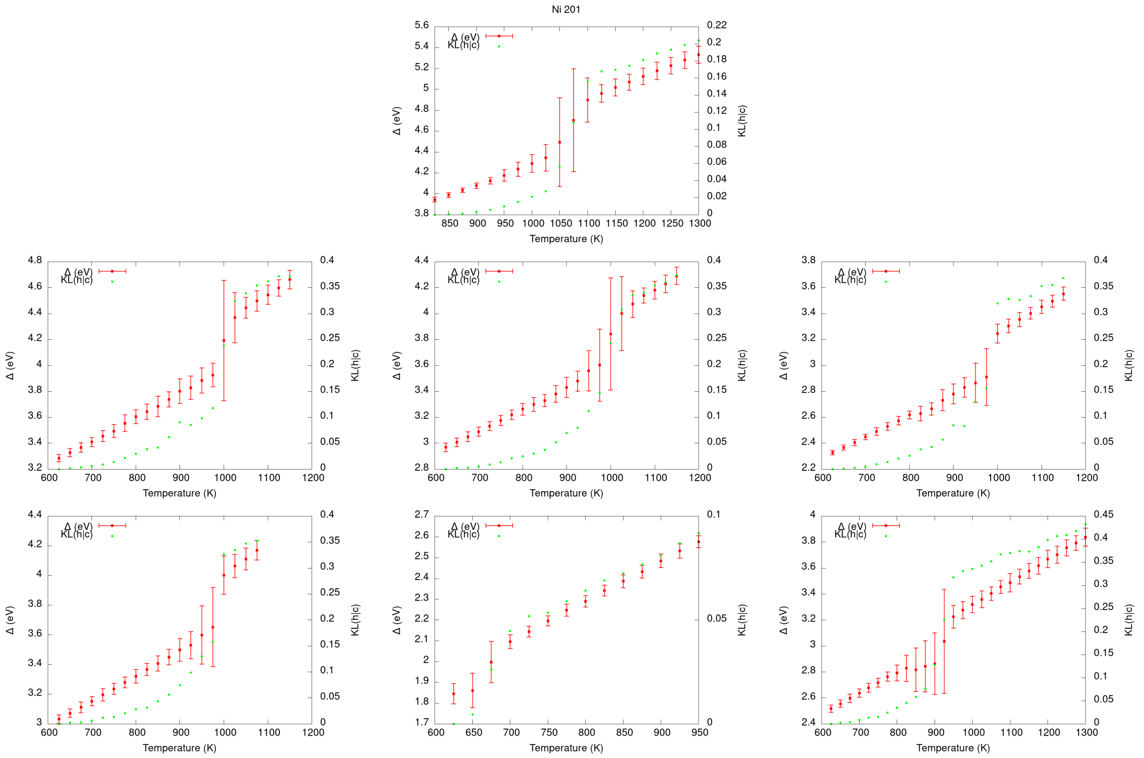

Figure S44: Excess energy and KL (h|c) temperature evolution in Ni systems with size 201 atoms in environments with different interaction strength and nature. The top central figure is Ni_{201} without environment, shown as reference. The phase change shifts towards colder temperatures with an increasing interaction.

S10.4 Gold

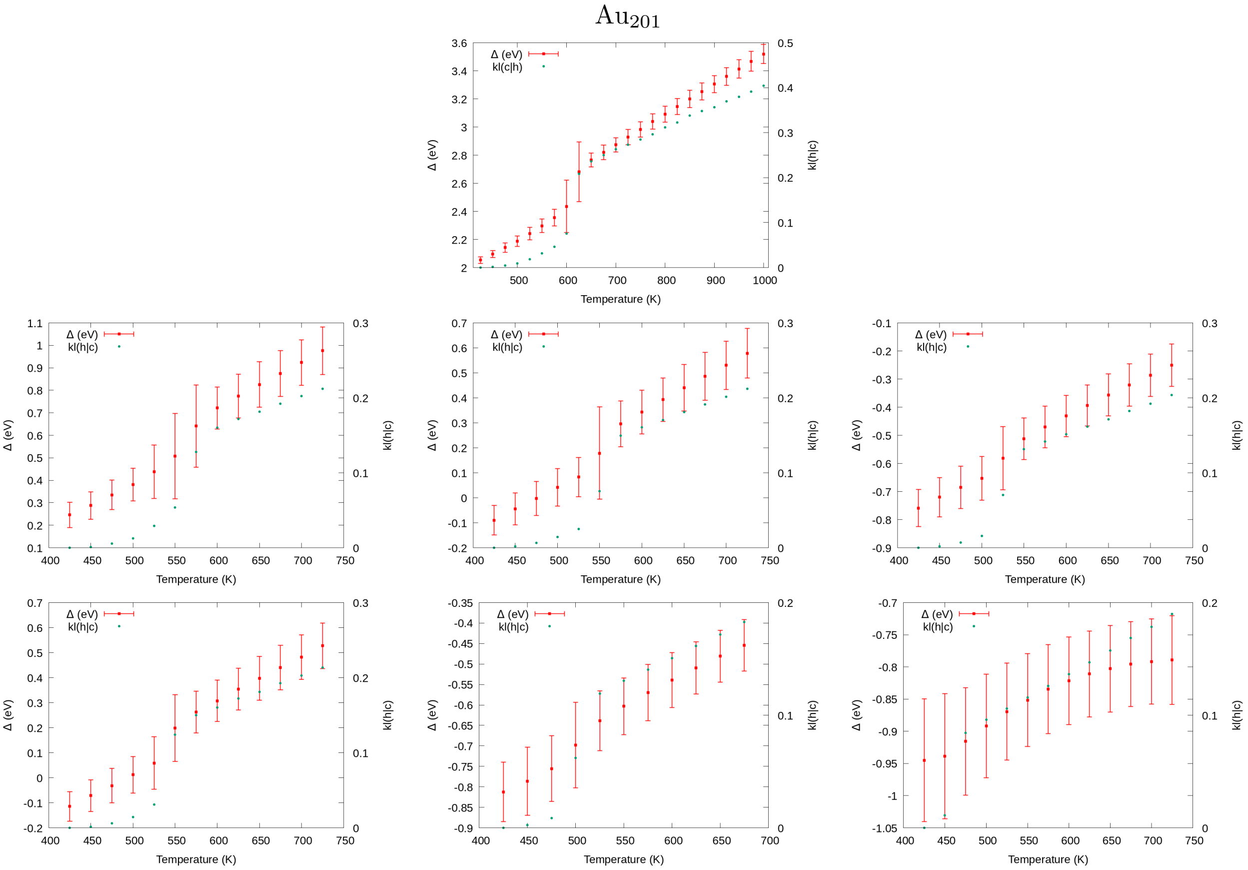

Figure S45: Excess energy and KL (h|c) temperature evolution in Au systems with size 201 atoms in environments with different interaction strength and nature. The top central figure is Au$_{201}$ without environment, shown as reference. The phase change shifts towards colder temperatures with an increasing interaction.

S10.5 Silver

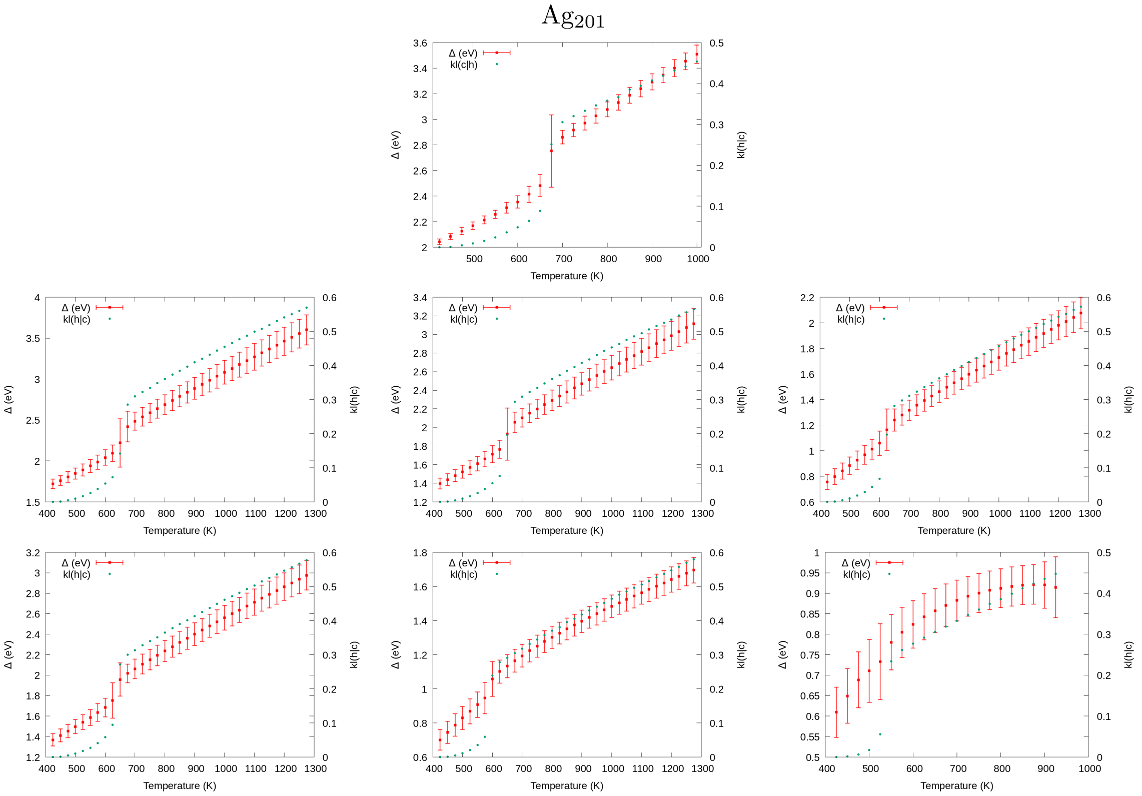

Figure S46: Excess energy and KL (h|c) temperature evolution in Ag systems with size 201 atoms in environments with different interaction strength and nature. The top central figure is Ag$_{201}$ without environment, shown as reference. The phase change shifts towards colder temperatures with an increasing interaction.

S10.6 Copper

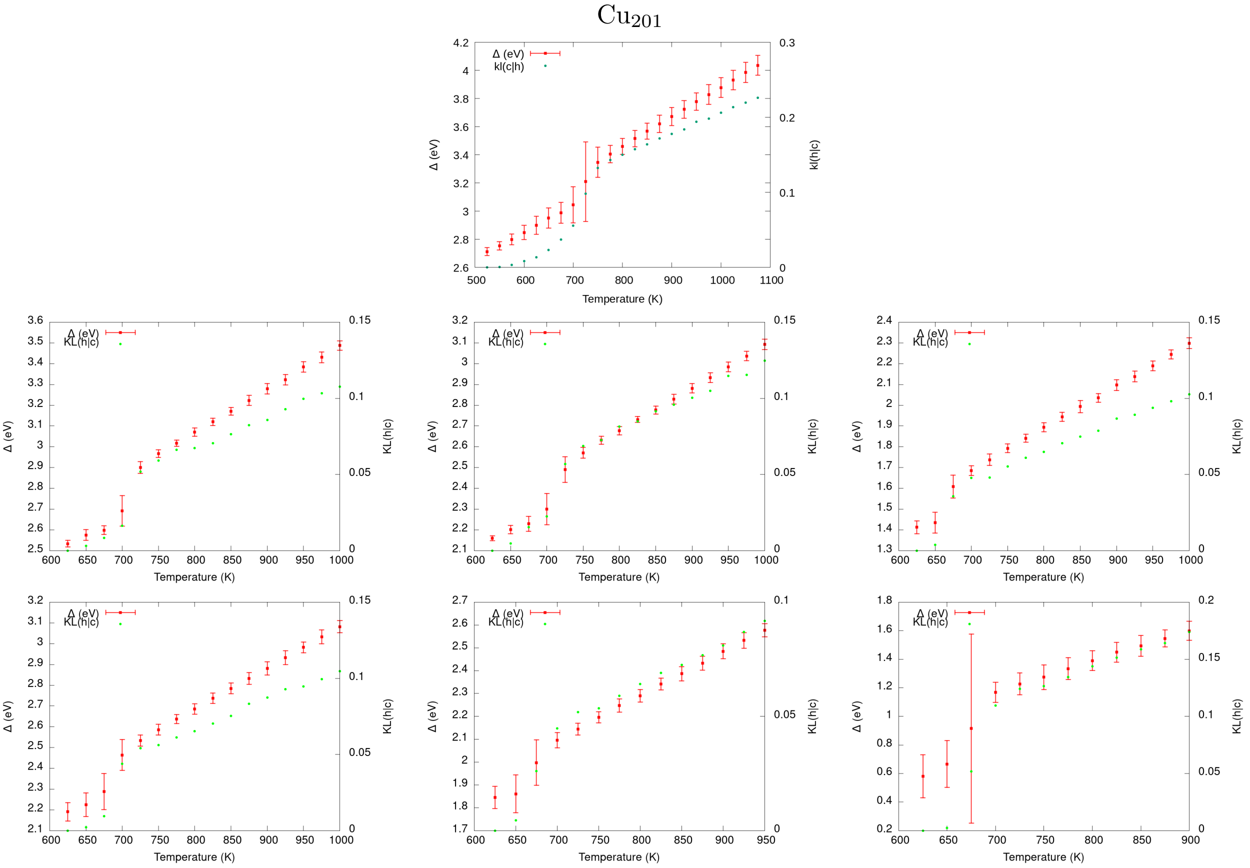

Figure S47: Excess energy and KL (h|c) temperature evolution in Cu systems with size 201 atoms in environments with different interaction strength and nature. The top central figure is Cu_{201} without environment, shown as reference. The phase change shifts towards colder temperatures with an increasing interaction.